



January 2019

Determination Of Sorption Characteristics Of Wood Using A New Non-Fickian Empirical Model

Joshua Troy Hatton

[How does access to this work benefit you? Let us know!](#)

Follow this and additional works at: <https://commons.und.edu/theses>

Recommended Citation

Hatton, Joshua Troy, "Determination Of Sorption Characteristics Of Wood Using A New Non-Fickian Empirical Model" (2019). *Theses and Dissertations*. 2560.
<https://commons.und.edu/theses/2560>

This Thesis is brought to you for free and open access by the Theses, Dissertations, and Senior Projects at UND Scholarly Commons. It has been accepted for inclusion in Theses and Dissertations by an authorized administrator of UND Scholarly Commons. For more information, please contact und.common@library.und.edu.

DETERMINATION OF SORPTION CHARACTERISTICS OF WOOD USING A NEW
NON-FICKIAN EMPIRICAL MODEL

by

Joshua Troy Hatton
Bachelor of Science, Bemidji State University, 2016

A Thesis
Submitted to the Graduate Faculty

of the

University of North Dakota
in partial fulfillment of the requirements

for the degree of

Master of Science


Grand Forks, North Dakota

August

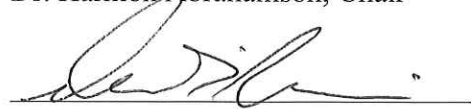
2019

Copyright 2019 Joshua Hatton

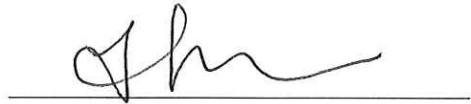
This thesis, submitted by Joshua T. Hatton in partial fulfillment of the requirements for the Degree of Master of Science from the University of North Dakota, has been read by the Faculty Advisory Committee under whom the work has been done and is hereby approved.



Dr. Harmon Abrahamson, Chair



Dr. David Pierce



Dr. Julia Zhao

This dissertation is being submitted by the appointed advisory committee as having met all of the requirements of the School of Graduate Studies at the University of North Dakota and is hereby approved.



Chris Nelson
Dean of the School of Graduate Studies

7/12/19

Date

PERMISSION

Title	Determination of Sorption Characteristics of Wood Using a New Non-Fickian Empirical Model
Department	Chemistry
Degree	Master of Science

In presenting this thesis in partial fulfillment of the requirement for a graduate degree from the University of North Dakota, I agree that the library of this University shall make it freely available for inspection. I further agree that permission for extensive copying for scholarly purposes may be granted by the professor who supervised my thesis work or, in his absence, by the chairperson of the department or the dean of the graduate school. It is understood that any copying or publication or other use of this thesis or part thereof for financial gain shall not be allowed without my written permission. It is also understood that due recognition shall be given to me and the University of North Dakota in any scholarly use which may be made of any material in my thesis.

Joshua T. Hatton
5/9/19

TABLE OF CONTENTS

TABLE OF CONTENTS.....	v
ABBREVIATIONS	ix
LIST OF FIGURES	x
LIST OF TABLES	xii
ACKNOWLEDGEMENTS.....	xiii
ABSTRACT.....	xv
CHAPTER I. INTRODUCTION.....	1
I.1 Wood absorption	1
I.2 Fickian versus empirical modelling.....	3
I.3 Construction of an empirical model	7
I.4 Various approaches to sigmoidal models	8
CHAPTER II. THE EFFECT OF PAINT ON WATER VAPOR ABSORPTION AND ¹⁴ C-TEBUCONAZOLE LEACHING	11
II.1 Materials.....	11
II.1.1 Chemicals	11
II.1.2 Wood treatment	12
II.1.3 Liquid scintillation counting	12
II.2 Exposure conditions	13

II.3 Method development of ^{14}C -extraction from simulated humidity chamber	14
II.4 Extraction and analysis	16
II.4.1 Water samples	16
II.4.2 Acetone samples.....	16
II.5 Estimate of maximum water uptake and half saturation time.....	16
II.6 Results and Discussion.....	17
II.6.1 Gravimetric analysis of water vapor adsorption.....	17
II.6.2 Optimization of ^{14}C -TAZ extraction	20
II.6.3 ^{14}C -TAZ depletion.....	21
II.6.4 Diffusion coefficients comparison	23
II.6.5 Comparison of different wood batches separated by time	25
II.6.6 Comparison to double reciprocal calculations	26
II.7 Conclusion.....	27
 CHAPTER III. GRAVIMETRIC ANALYSIS OF LIQUID WATER ABSORPTION.....	 29
III.1 Materials	29
III.2 Exposure conditions.....	29
III.3 Full factorial design	29
III.4 Nonlinear regression calculations of $T_{1/2}$ and $\text{H}_2\text{O}_{\text{max}}$	30
III.5 Statistical analysis.....	30
III.6. Results and discussion	30
III.6.1 $\text{H}_2\text{O}_{\text{max}}$ factors	32

III.6.2 $T_{1/2}$ factors	33
III.6.3 Multiple steps of diffusion	35
III.6.4 Comparison to double reciprocal calculation	36
III.7. Conclusion	37
CHAPTER IV. ABSORPTION OF VARIOUS SOLVENTS INTO A WOOD MATRIX	39
IV.1 Materials	39
IV.2 Exposure conditions	39
IV.3 Estimation of maximum solvent uptake and half saturation time	40
IV.4 Results and discussion	40
IV.5 Conclusion	41
CHAPTER V. CONCLUSIONS	42
APPENDICES	44
Appendix A – Algebraic proof of solving diffusion coefficients from empirical model	44
Appendix B – Individual Minitab for paint results	45
Appendix C – General linear model of H_2O_{max} with Tukey comparison	56
Appendix D – Average Minitab results for density and temperature	58
Appendix E – One-way ANOVA analysis of $T_{1/2}$ with Tukey comparison	66
Appendix F – Averaged saturation plots	67
Appendix G – Individual Minitab results for water and organic solvents	68

REFERENCES 71

ABBREVIATIONS

ACS – American Chemical Society

DPM – Disintegrations per minute

EMC – Equilibrium moisture content

FSP – Fiber saturation point

H_2O_{max} – Maximum amount of water absorbed

IUPAC- International Union of Pure and Applied Chemistry

K_M – substrate concentration to reach half V_{max}

LLEH – Liquid–liquid extraction with hexane

SC – Scintillation cocktail

$T_{1/2}$ – Time to reach half H_2O_{max}

TAZ – Tebuconazole

V_{max} – Maximum rate

VOCs – Volatile organic compounds

LIST OF FIGURES

Figure 1. Left: Equilibrium moisture content of wood (labeled contours) as a function of temperature and relative humidity. Right: Moisture content and relative humidity relationship for wood under various sorption conditions. ³ [Copied from <i>Wood Handbook – Wood as an Engineering Material</i> (2010), U.S. Department of Agriculture. Figures 4-1 and 4-2.]	2
Figure 2. Ideal model diffusion.....	5
Figure 3. Sigmoidal curves via various formulas.	8
Figure 4. Example of Michaelis-Menten and Lineweaver-Burk plots. Data taken from Ritchie, et al. ²⁰	9
Figure 5. Schematic of liquid scintillation counter.....	13
Figure 6. Schematic of humidity chamber.....	14
Figure 7. H_2O_{max} and $T_{1/2}$ values. Error bars are one standard deviation	19
Figure 8. Comparison of extraction techniques on samples.	21
Figure 9. Sum of water and acetone ^{14}C -TAZ washes. Left display shows individual measurements. Right side display accumulative.	22
Figure 10. Comparison of solved diffusion coefficients for both Fickian and Empirical models.....	24
Figure 11. Comparison of old and new samples.....	26
Figure 12. Double reciprocal plot of Clear Prime and Clear Paint (prime and top-coat).	27

Figure 13. Accumulative weight versus time. Left, low density & right, high density. Error bars are one standard deviation.	31
Figure 14. Normal plot, normal probability plot, versus fits, and main effects plots for H_2O_{max}	33
Figure 15. Normal plot, normal probability plot, versus fits, and interval plot plots for $T_{1/2}$	34
Figure 16. Double reciprocal plot of High density - low temperature.	36
Figure 17. Saturation graphs of water, <i>n</i> -hexadecane, and Woodlife. a) Comparison of all three. b) Zoomed in section comparing <i>n</i> -Hexadecane and Woodlife. c) Comparison of water and <i>n</i> -hexadecane.	41

LIST OF TABLES

Table 1. Protocols tested for ^{14}C -TAZ extraction.	14
Table 2. Summary of $\text{H}_2\text{O}_{\text{max}}$ and $\tau_{1/2}$. Following the value is the standard error calculated in Minitab. Any 0.00 standard error should be considered as <0.001	18
Table 3. Comparison of nonlinear regression and double reciprocal calculations.	27
Table 4. Full factorial design.	30
Table 5. Raw results of nonlinear regression calculations.	31
Table 6. Analysis of variance for $\text{H}_2\text{O}_{\text{max}}$ versus density and temperature.	32
Table 7. Analysis of variance for $\tau_{1/2}$ versus temperature.	34
Table 8. $\text{H}_2\text{O}_{\text{max}}$ and $\tau_{1/2}$ averaged values for all conditions. No standard deviations were greater than 10^{-5} for $\text{H}_2\text{O}_{\text{max}}$ and were consequently omitted.	35
Table 9. Comparison of $\text{H}_2\text{O}_{\text{max}}$ and $\tau_{1/2}$ via nonlinear regression and double reciprocal calculations. Standard deviation for $\text{H}_2\text{O}_{\text{max}}$ nonlinear regression was greater than 10^{-5} and was consequently omitted.	37
Table 10. Results of nonlinear regression.	41

ACKNOWLEDGEMENTS

I would like to thank Dr. Harmon Abrahamson for his willingness to guide me through the final chapter of my graduate career; without his guidance and support I am positive that I would not have finished my studies. I also greatly appreciate both Dr. David Pierce and Dr. Julia Zhao for their contributions as members in my committee and as excellent teaching professors; both of their classes were instrumental in how chemistry problems should be approached and thought about.

I am very fortunate to have worked with many great graduate students, including, Solene Bechelli, Brett Nespor, Audrey LaVallie, Jan (Honza) Belík, Jana Rousova, Anastasia Andrianova, Klara Kukowski, and Josh Schumaker. Moreover, I would like to thank the undergraduates that I worked with; Natalie Stjernen, Paul Schoenberger, and Cole Stevens. I would also like to thank Dr. Martin Halecky and Jan (Honza) Chalupa for their mentorship during my brief studies in the Czech Republic and the IRES program for making it possible.

I am very appreciative to Steve Fisher of Marvin Windows and Doors for their financial support of my thesis over the years. I would also like to thank Klara Kukowski and Ganna Baglayeva for their previous works contributing to Chapter IV of this thesis.

I would like to thank the University of North Dakota, the Chemistry Department, and the Graduate School for giving me the opportunity to pursue graduate studies. I would also like to thank the University Counseling Center; they are an underappreciated resource and certainly deserve more recognition than they currently get.

For all of the suggestions and advice that Dr. Kubátová and Dr. Koziak provided to me, in an unwavering fashion, I extend my sincerest acknowledgement. During our numerous meetings, they counseled me on topics that ranging from lab techniques, to analysis, and any known scenario. Knowledgeably and passionately they both joined me on my journey, and for that I say thank you.

I would like to thank my family and friends. My parents, Ross and Jennifer, have supported me every step of the way. As well as my five younger brothers: Mickenzie, Charlie, Jack, Garrett, and Sawyer. I extend a very special thanks to Mathew Steichen and Avery Franzen; though they may be at different schools and programs, their insights were always scholarly.

Finally, I give the upmost thanks to my girlfriend, Billigene. Her unconditional love, encouragement, and support made all of this possible.

ABSTRACT

Wood is a versatile and cost-effective building material found in everyday life. However, it has a disadvantage of readily absorbing both water vapor from the surrounding air and liquid water when in direct contact. The absorption of water increases the rate of the wood decaying and can also affect the physical properties, such as warping and swelling. Previous research has looked into defining the rate of absorption by modeling it based on Fick's second law. Fick's second law bases the rate of absorption on a diffusion coefficient; a constant that changes with time. Herein, a new empirical model is proposed that has constants that stay fixed with time as a way to avoid using diffusion coefficients. Furthermore, the empirical model's validity will be examined for water vapor and the effect of paint coatings, liquid water at different wood densities and temperature, and the application of the model to organic solvents.

CHAPTER I. INTRODUCTION

I.1 Wood absorption

The International Union of Pure and Applied Chemistry (IUPAC) defines absorption as the process of one material being retained by another by physical forces.¹ For most cases, this is the study of a dissolved solid, liquid, vapor, or gas being bound throughout a solid. This is an important distinction from adsorption, which only takes place on the surface of a solid. Conversely, because absorption is a physical process, there can also be desorption; in which the retained material is released. In general, both absorption and desorption can be described as the single process of sorption. Many materials exhibit sorption, including activated carbon, various media gels, and zeolites.² However, the most abundant material is one that is used in nearly every building and found in copious amounts in nature: wood.

Wood is a common material used by nearly everyone on a daily basis; window frames, desks, house frames, doors, and dressers to name a few. There are many advantages to using wood as a building material as it is plentiful, inexpensive, easy to cut and shape, and is considered a green, renewable material. However, wood does have the property of absorbing both liquid water and water vapor, which can accelerate the rate at which it decays.

The absorption of water vapor is a process that proceeds towards equilibrium that is both temperature and relative humidity dependent.³ This final absorption value is commonly referred to as equilibrium moisture content (EMC) and has different values with each species of wood. Furthermore, EMC exhibits a hysteresis phenomenon, in which EMC values are higher when desorption occurs after an initial absorption (Figure 1). Overall, water vapor sorption is a relatively slow process that takes days to reach equilibrium.

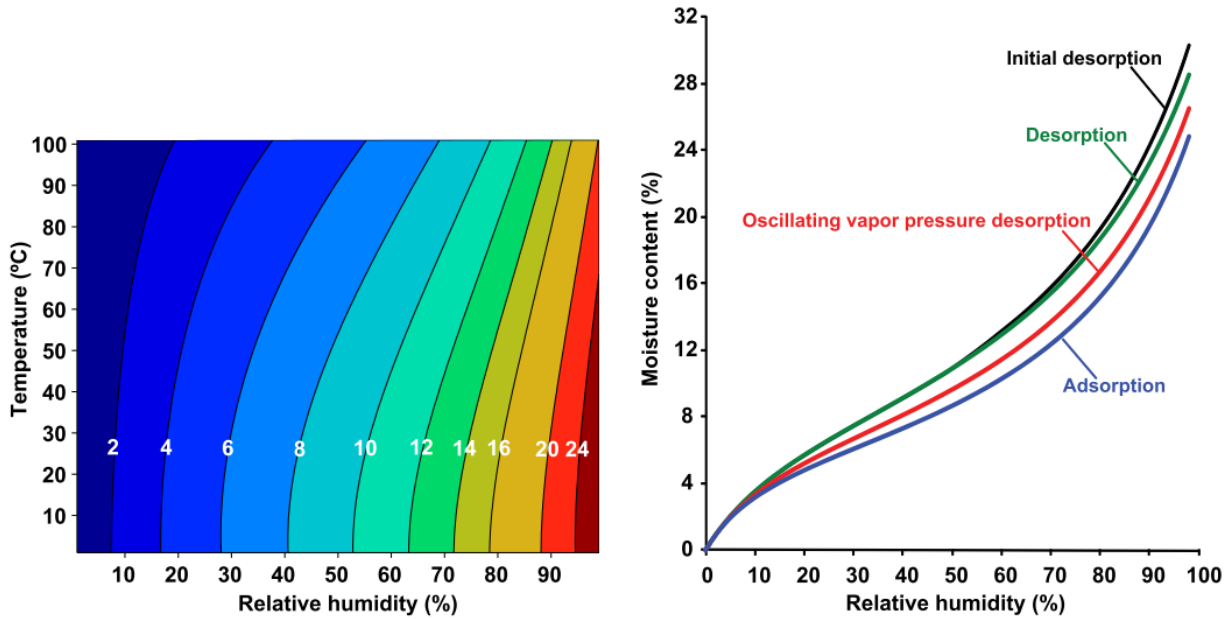


Figure 1. Left: Equilibrium moisture content of wood (labeled contours) as a function of temperature and relative humidity. Right: Moisture content and relative humidity relationship for wood under various sorption conditions.³ [Copied from *Wood Handbook – Wood as an Engineering Material* (2010), U.S. Department of Agriculture. Figures 4-1 and 4-2.]

Compared to water vapor, liquid water absorption is a significantly faster process and has multiple mechanisms of absorption. The primary mechanism is driven by capillary action, also known as wicking, that happens within the xylem and phloem channels inherent in the wood. Consequently, the penetration of absorption goes much farther along these channels and much less perpendicular to them.^{3,4}

The way in which wood sorbs both water vapor and liquid is categorized by bound water and free water.^{3,5} Bound water is defined by having an intermolecular attraction to the cellulose found in the cell walls and the point at which all available bonding sites are full is referred to the fiber saturation point (FSP).⁶ Free water is all other water that is not bound to the cell walls and only occurs after the FSP has been reached.⁵ In the case of water vapor, free water does not occur

as the vapor cannot “push” past the FSP. Moreover, the rate of both water vapor and liquid water absorption predictably changes while reaching the FSP; and in the case of liquid water, experiences another rate change after the FSP.

To better understand how wood absorption is occurring, various models have been developed. The two main approaches to developing these models is based on mathematical derivation of physics concepts or through experimental data to build an empirical model. Both of these approaches will be explored in the following section.

I.2 Fickian versus empirical modelling

Most of the models describing diffusion (absorption) of water in wood are Fickian (i.e., they follow Fick’s Law), as this is a traditional treatment based on sound physics of diffusion.^{7–12} However, the Fickian model assumes constant diffusion coefficients over specific time frames, and this is not observed in real measurements. Absorption must, and does, reach a near-zero rate as equilibrium is reached and the main diffusion paths become filled.^{3,4,7–10,12–15}

The general diffusion constant equation for a non-steady state, one-dimensional analysis is defined by Fick’s second law (Eq.1). This equation relates the rate of change in concentration (weight) with respect to the time between parallel planes at points x and $x + dx$.

$$\frac{\partial C}{\partial t} = D \frac{\partial^2 C}{\partial x^2} \quad \text{Eq. 1}$$

The solutions of Fick’s second law are based on a set of boundary conditions and have been used in similar studies.^{4,8,9,13,14,16,17} When measuring diffusion by mass uptake bounded by two parallel planes, Eq. 1 can be solved to result in Eq. 2.

$$\frac{w_t - w_0}{w_\infty - w_0} = 1 - \frac{8}{\pi} \sum_{n=0}^{\infty} \frac{1}{(2n+1)^2} e^{-D(2n+1)^2 \pi^2 t / L^2} \quad \text{Eq. 2}$$

where W_t is the weight (g) at time t (min), W_∞ is the weight at time infinity, W_0 is the initial weight, L is the length of the wood block, and D is diffusion (m^2/min). For short time spans and rectangular blocks of wood, Eq. 2 can be simplified to Eq. 3.^{4,12}

$$\frac{w_t - w_0}{w_\infty - w_0} = \frac{2}{\sqrt{\pi}} \left(\frac{A}{V} \right) \sqrt{Dt} \quad \text{Eq. 3}$$

where A is the surface area (m^2) and V is the volume (m^3) that is exposed to water vapor. $A = 2(wl + hl + hw)$ and $V = hwl$. By redefining $W_t - W_0$ and $W_\infty - W_0$ as $H_2O_{(t)}$ and H_2O_{max} , respectively, Eq. 3 can be rearranged to give an equation that describes water uptake at time (t) if both the H_2O_{max} and diffusion constant are known (Eq. 4).

$$H_2O_{(t)} = H_2O_{(max)} \frac{2}{\sqrt{\pi}} \left(\frac{A}{V} \right) \sqrt{Dt} \quad \text{Eq. 4}$$

where H_2O_{max} is the maximum amount of absorption that is eventually achieved from the equilibrium process. With this equation, the diffusion constant is constantly changing with time in order to match real measurements (Figure 2). Initial diffusion is rapid until it peaks and then begins to slow down to essentially zero. This poses a rather difficult problem of finding meaning out of a diffusion coefficient, as it changes either rapidly or infinitesimally depending on the length of time and makes H_2O_{max} difficult to know or predict without doing it experimentally. Furthermore, the time in which it takes to reach H_2O_{max} is only defined via the diffusion coefficients, which for reasons previously mentioned, are not ideal.

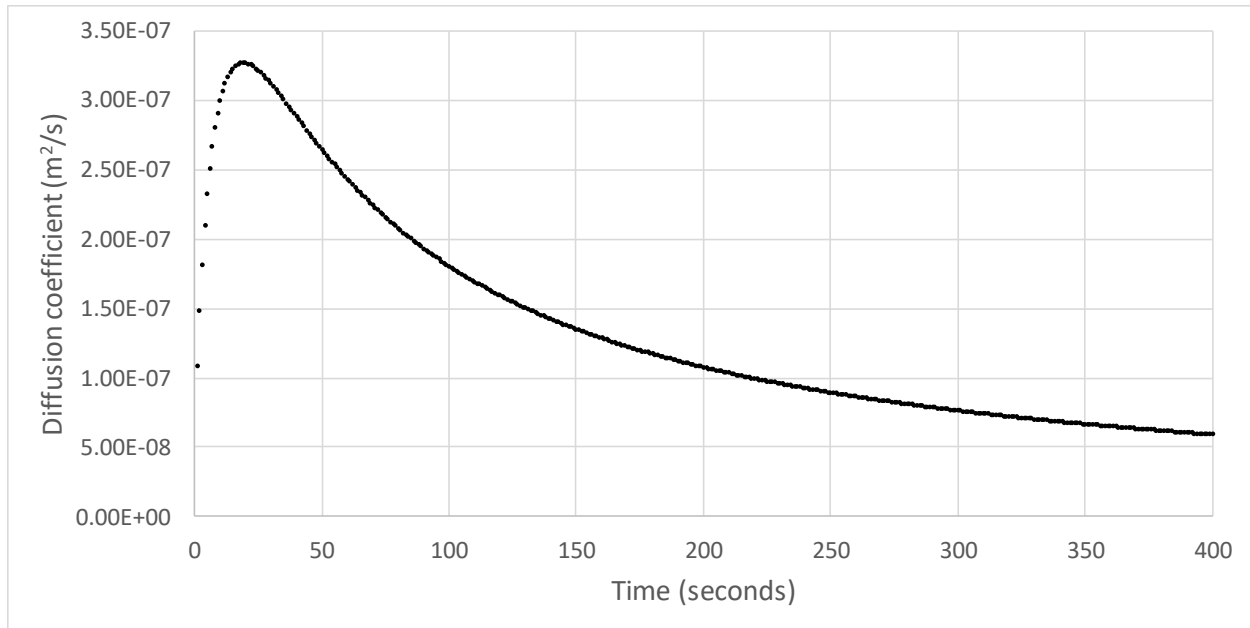


Figure 2. Ideal model diffusion.

The current traditional adjustment of the Fickian model to this scenario is to use several constant diffusion coefficients for several phases of diffusion.^{4,12} However, this treatment sets significant limitations. First, the abrupt switches from one phase to another are set arbitrarily. Second, it assumes that all samples will show the same number of phases, which may not be true. Third, the actual changes of diffusion rates are gradual and continuous, contradicting the idea of several distinct phases. Fourth, having several drastically different values of diffusion coefficients, as it is inherent for wood, hinders accurate modelling.

As a result, the predictability of Fickian models is limited to systems exhibiting similar diffusion features, e.g., wood samples obtained from one batch, with a similar extent of drying and just one diffusing chemical or their defined mixture.^{3,9,18} The targeted use of both painted and

unpainted samples, varied pollutants, and even their varied physical phase (vapor versus liquid) would be inconsistent with this approach.

However, the alternate use of empirical, non-Fickian models has even greater limitations. For example, Baglayeva, et al., incorporated new empirical constants based on drying the wood with high temperatures, which can further increase the variability between measurements as wood extracts could be evaporated from the wood.¹² Other works, such as those of Murr, et al., and Wadsö, focus on modeling slow and fast steps of sorption based on fitting exponential equations.^{13,17} They may offer an advantage of using fewer parameters (ideally – just one) to describe the entire time-course of absorption of a chemical by a matrix. However, as these empirical equations are not based on sound physical laws, their predictability to even slightly differing systems is questionable at its basis.

Thus, the ideal case would be finding an empirical model with continuously decreasing diffusion rates that would still be reconcilable with the Fickian model. In the ideal case, such a model would describe the entire process, although having several phases, each corresponding to a different physical process (e.g., capillary action vs. molecular diffusion), could be acceptable.

I.3 Construction of an empirical model

As previously mentioned, the current Fickian model (Eq. 3) has several issues. The significant ones that have the potential to be addressed by an empirical model are replacing diffusion coefficients with a different constant and potentially predicting H_2O_{max} . In order to do so, we propose incorporating a new constant that defines the time it takes to reach half-saturation, $\tau_{1/2}$, which can be seen in Equation 5.

$$H_2O_{(t)} = H_2O_{(max)} \left(\frac{t}{\tau_{1/2} + t} \right) \quad \text{Eq. 5}$$

There are several advantages to using this empirical equation. First, from experimental data it creates the same saturation curves as Fick's second law (Eq. 3). Second, $\tau_{1/2}$ replaces the diffusion coefficient; this is advantageous because it does not change with time. Moreover, $\tau_{1/2}$ has only units of time, which is straightforward compared to diffusion's meters squared per time. Lastly, as the two equations are set to be equal to each other, diffusion coefficients can still be calculated if desired from Equation 6.

$$D = \frac{t\pi V^2}{4(\tau_{1/2} + t)^2 A^2} \quad \text{Eq. 6}$$

In the following chapters, this empirical model will be tested in various conditions. For the first circumstance, the simplest absorption system of water vapor will be evaluated, including the effect that paint has on its absorption. Secondly, liquid water absorption will be evaluated. Furthermore, the effect of the wood's density and the temperature of the water and their interactions will be statistically analyzed to see what effect they may have on H_2O_{max} and $\tau_{1/2}$. Lastly, the application of the model to other, non-polar, chemicals will be assessed.

I.4 Various approaches to sigmoidal models

Both Fick's second law and the empirical model describe the positive portion of a sigmoidal curve. However, there are many examples of chemical and physical systems that exhibit this kind of trend; including Michaelis-Menten enzyme kinetics, Fermi-Dirac statistics, Weibull distributions, and steady-state chemical reactions, to name a few. Moreover, with these different applications come different, yet similar, mathematical ways to describe these curves (Figure 3).

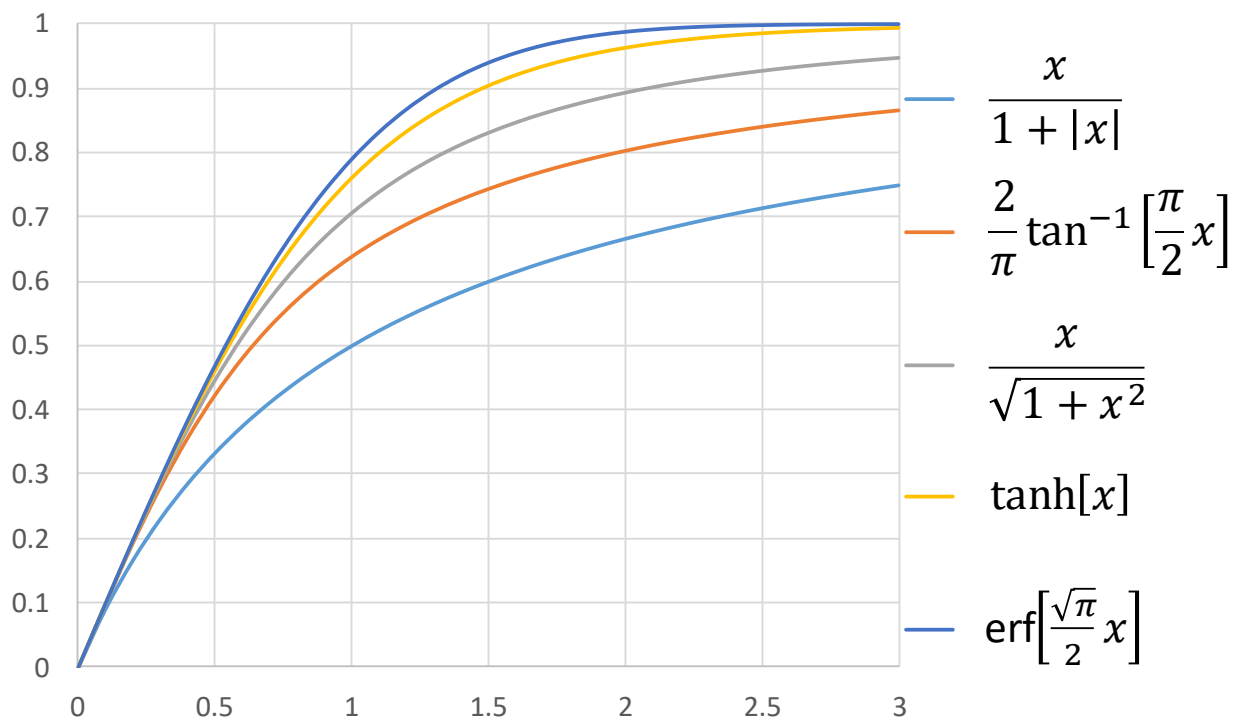


Figure 3. Sigmoidal curves via various formulas.

Most of the equations seen in Figure 3 are abstract in the realm of chemistry, with the exception of the first. This equation is the same format as the Michaelis-Menten equation and has been used to describe the factors of max rate (V_{\max}) and concentration required to reach half that

maximum rate (K_M).¹⁹ However, the way to calculate these constants has been demonstrated to be problematic before the advent of adequate computational methods (i.e., nonlinear regression).²⁰ One common approach to solve for these constants was to make a double reciprocal plot of the Michaelis-Menten graph, commonly referred to as a Lineweaver-Burk plot (Figure 4).

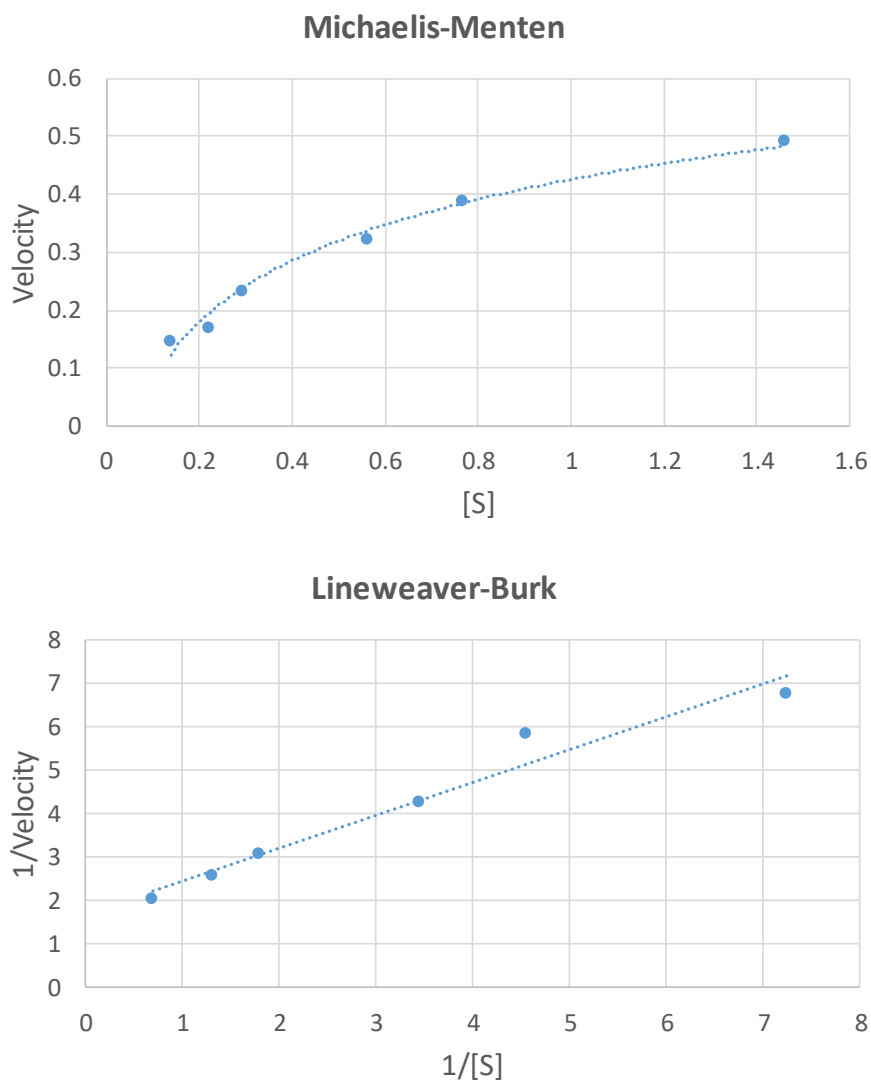


Figure 4. Example of Michaelis-Menten and Lineweaver-Burk plots. Data taken from Ritchie, et al.²⁰

The linearization provided by Lineweaver-Burk plots, and other similar transformations, has demonstrated the capability of calculating constants with more ease than from the original Michaelis-Menten formula. Unfortunately, each of these transformations has the disadvantage of being more inaccurate at smaller values, due to the nature of taking the inverse of a small number. Therefore, having inaccurate or imprecise measurements at the start of an experiment can cause the resulting constants to be significantly incorrect. Fortunately, nonlinear regression can be applied directly to Michaelis-Menten plots and used to calculate the constants without having to transform the data, resulting in an overall more accurate result.²⁰ Therefore, all the cases of water absorption, and the application of the empirical model, will be evaluated by nonlinear regression.

CHAPTER II. THE EFFECT OF PAINT ON WATER VAPOR ABSORPTION AND ¹⁴C-TEBUCONAZOLE LEACHING

As water vapor only has one step of absorption that takes place within wood, it makes logical sense to see if the empirical model can work in this simple system. Furthermore, in association with Marvin Windows & Doors, the effect of various paints was evaluated to see if they had an impact on the water vapor absorption. The effect of paint and the rate of which radiolabeled fungicide was leached was also monitored. Previous work had shown that painted wood that was exposed to simulated rain demonstrated that both the maximum amount and the rate of fungicide leaching was reduced.²¹ However, the effect of water vapor and leaching had not been explored.

II.1 Materials

II.1.1 Chemicals

Uniformly ¹⁴C-labeled tebuconazole (TAZ) was obtained from the Commerce Institute of Isotopes Co., Ltd. (Budapest, Hungary) with a radioactivity of 7.4 MBq mL⁻¹, which was added to a commercial wood preservative formulation, Woodlife 111 TRU from Kop-Coat, Inc. (Pittsburgh, PA, USA) as a tracer; resulting in a radioactivity of 0.74 MBq L⁻¹ and ¹⁴C-TAZ concentration of 0.12 mg L⁻¹. Woodlife 111 additionally contains 0.21% of nonradioactive TAZ, propiconazole, and 3-iodo-2-propynylbutylcarbamate. Thus, the ratio of ¹⁴C-TAZ to TAZ was 1:14,000. Two different scintillation cocktails were used. Betamax, obtained from MP Biomedicals, LLC (Solon, OH, USA), and Ultima Gold, obtained from PerkinElmer, Inc. (Waltham, MA, USA), were used for organic and aqueous solvents, respectively. Acetone (ACS grade) was purchased from VWR (Arlington Heights, IL, USA). Sodium bromide (99+%) and

potassium iodide (99%) were purchased from Alfa Aesar (Haverhill, MA, USA). All water used was deionized water from a Direct-Q 3 UV system purifier (Millipore, Billerica, MA, USA).

II.1.2 Wood treatment

Ponderosa pine sapwood blocks (4 in x 1 in x 0.5 in) were dip treated with a radiolabeled Woodlife 111 solution for 1.0 min. The wood blocks were then dried on wooden skewers in a hood for a week before being painted. Samples were weighed 13 days after initial Woodlife treatment and priming/painting for their initial weight.

II.1.3 Liquid scintillation counting

The liquid scintillation counter used was a Beckman Coulter LS 6500 purchased from Beckman Coulter, Inc. (Fullerton, CA, USA). The analyses were run in duplicate for 10.0 min in disintegrations per minute (DPM) mode, which is directly proportional to the ^{14}C -TAZ concentration.

Liquid scintillation counting is based on a principle that is similar to any luminescence technique. For example, fluorescence occurs after exciting a fluorophore with an incident beam of light, followed by the excited molecule returning to the ground and emitting light. For liquid scintillation counting, the incident light source is replaced with a radiation source (specifically ^{14}C beta radiation for this experiment). Then rather than the fluorophore being excited directly, the beta particles excite the SC, which then transfers that energy to the fluorophore. The now excited fluorophore will return to the ground state and give off photons, which are detected by a photomultiplier tube (Figure 5).^{22,23} The amount of fluorescence is proportional to the amount of beta-emitting isotope present. Beta radiation from ^{137}Cs was used for standardization.

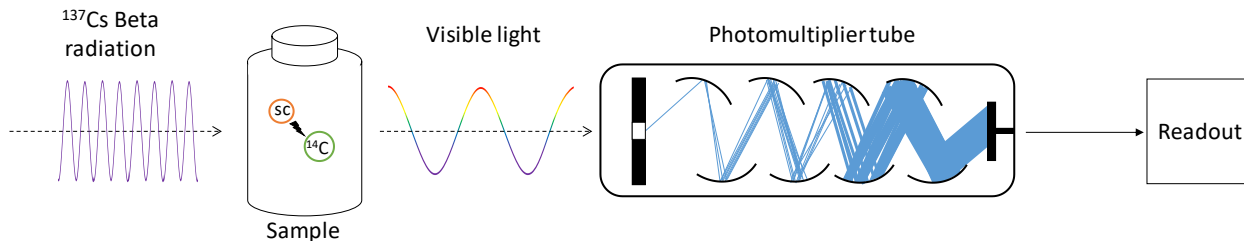


Figure 5. Schematic of liquid scintillation counter.

II.2 Exposure conditions

A saturated salt solution of sodium bromide or potassium iodide was utilized to keep a constant relative humidity (~60%) at room temperature and 65 °C, respectively, inside a glass jar, Figure 6. The wood blocks were then placed on top of a perforated plastic platform with no direct contact to the salt solution below. Gravimetric measurements were taken weekly for the first three weeks and biweekly for the last two measurements, for a total water vapor exposure of 52 days.

The remaining solution inside the chambers was collected at the same time as gravimetric measurements to measure the rate of ^{14}C -TAZ depletion. The chambers were rinsed several times with acetone to collect any residual ^{14}C -TAZ. Lastly, the humidity chambers were washed and refilled with the saturated salt solution and wood blocks were reintroduced to continue the experiment.

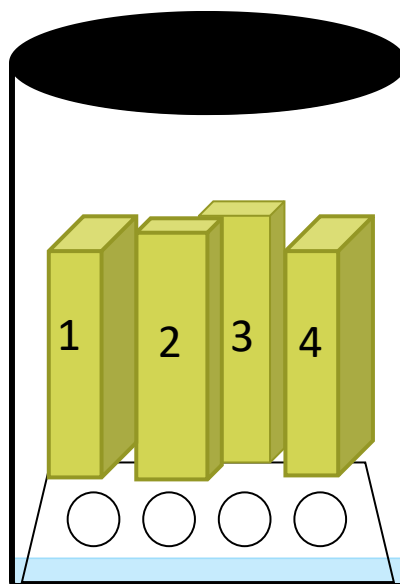


Figure 6. Schematic of humidity chamber.

II.3 Method development of ^{14}C -extraction from simulated humidity chamber

To simulate the water collected in the humidity chamber and assure recovery, several experimental designs were tested (Table 1). Each protocol tested used $5\ \mu\text{L}$ of ^{14}C -TAZ to verify recovery.

Table 1. Protocols tested for ^{14}C -TAZ extraction.

Sample	Protocol	Matrix	SC
Aqueous control	Aqueous samples	Water & sodium bromide	Ultima Gold
Organic control	Organic samples	Acetone	Betamax
Aqueous control	LLEH	Acetone	Betamax
Aqueous control + wood matrix	LLEH	Acetone & Wood matrix	Betamax

The protocol for aqueous samples included the same saturated salt solution used in a humidity chamber, ^{14}C -TAZ, and diluting it to 30 mL to dissolve excess salt. Next, aliquots of SC were separated with a ratio of 1:2 (H_2O :SC) and equilibrated for 3 days before being analyzed with the scintillation counter. The organic samples consisted of 2 mL acetone, 2 mL of SC, and the ^{14}C -TAZ.

Liquid–liquid extraction with hexane (LLEH) consisted of the same conditions as the direct water measurement, but was halted before addition to the SC. From there, ~4 mL of *n*-hexane was added and vortexed. The solution was allowed to separate into two layers and the top layer was transferred into a scintillation vial with a glass Pasteur pipette. Hexane was added, vortexed, and collected three times. The combined hexane fractions were then dried to completion under a gentle stream of nitrogen. Lastly, 2.0 mL each of acetone and SC were added and vortexed. This protocol was repeated with the addition of wood matrix present in a separate set of solutions to determine the effects of the sample matrix.

Wood matrix extract was obtained by performing Soxhlet extraction on untreated ponderosa wood block samples for 24 hours with acetone. A rotary evaporator was then used to concentrate the acetone to ca. 10 mL, which was then transferred to the vial used to simulate the humidity chamber, and dried to completion using nitrogen. The previously mentioned LLEH protocol was then performed and the sample vials were equilibrated overnight before being analyzed.

II.4 Extraction and analysis

II.4.1 Water samples

Water collected from the humidity chambers was diluted to 30 mL (to dissolve any excess salt) and ~4 mL of *n*-hexane were added and vortexed. The solution was allowed to separate into two layers and the top layer was transferred into a scintillation vial. Hexane was added, vortexed, and collected three times. The combined hexane fractions were then dried under a gentle stream of nitrogen till dry. Lastly, 2.0 mL of acetone and scintillation cocktail were added and vortexed. These samples then equilibrated over night before being run on the scintillation counter.

II.4.2 Acetone samples

The acetone rinsed samples collected from the humidity chambers were evaporated with a gentle stream of nitrogen until dry. After reconstitution with three 3 mL washes with acetone, they were transferred to scintillation vials. The acetone was dried under nitrogen to completion and reconstituted in 2.0 mL of acetone and scintillation cocktail were added and vortexed. The samples were allowed to equilibrate overnight before being analyzed with the scintillation counter.

II.5 Estimate of maximum water uptake and half saturation time

H_2O_{\max} and $T_{1/2}$ were solved using nonlinear regression in Minitab® Statistical Software²⁴ from the gravimetric measurements taken. Each wood sample was weighed weekly for three weeks and then every two weeks. The total exposure time was 52 days.

II.6 Results and Discussion

II.6.1 Gravimetric analysis of water vapor adsorption

The individual nonlinear confidence plots can be found in Appendix F. The calculated values for H_2O_{\max} and $\tau_{1/2}$ can be seen in Table 2.

Table 2. Summary of H_2O_{max} and $T_{1/2}$. Following the value is the standard error calculated in Minitab. Any 0.00 standard error should be considered as <0.001.

Paint coat	H_2O_{max}	$T_{1/2}$
Diamond Vogel SDL (one coat)	5.2 ± 0.21	3.6 ± 0.85
DBK (prime and top-coat)	4.9 ± 0.66	12.1 ± 4.83
White Painted Interior Finish (prime and top-coat)	3.8 ± 0.00	6.3 ± 0.00
White Painted Interior Finish (one coat)	5.0 ± 0.18	5.2 ± 0.89
Marvin White Prime (one coat)	4.5 ± 0.23	10.4 ± 1.66
Marvin Espresso Conditioner Stain and Clear Coat (prime and two top-coats)	4.3 ± 0.20	5.2 ± 1.11
Clear Prime and Clear Paint (prime and top-coat)	4.8 ± 0.29	7.8 ± 1.76
Sherwin Williams Exterior Paint (prime and top-coat)	4.7 ± 1.44	19.1 ± 14.70
Kilz Premium Extra Primer with Sherwin Williams Exterior Paint (prime and top-coat)	5.7 ± 0.19	8.7 ± 1.01
Benjamin Moore Superior Primer with Regal Exterior Paint (Prime and top-coat)	5.7 ± 0.57	8.1 ± 2.91
Control	4.6 ± 0.00	2.6 ± 0.06

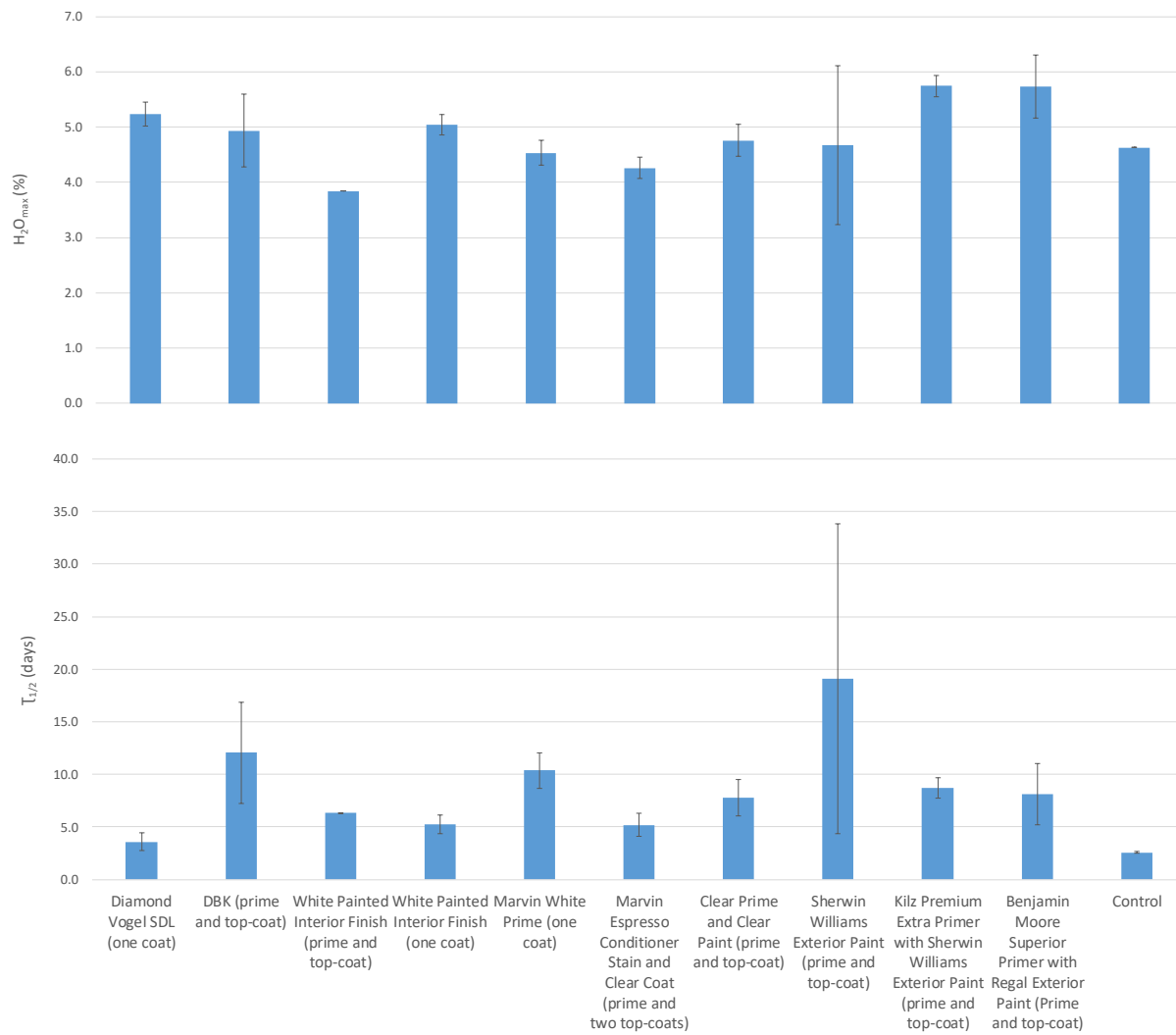


Figure 7. H_2O_{max} and $T_{1/2}$ values. Error bars are one standard deviation.

Each paint coat observed a statistically significant increase in H_2O_{max} when compared to the control; with an average increase of ~30% (Figure 7). It could be proposed that the increase of water absorbed could be contained in the paint itself but a method of ascertaining it would be difficult to develop. The process of removing the paint from the wood by either physical or chemical methods, without losing water, is currently not available.

$T_{1/2}$ is also increased by the addition of paint and varied significantly between the different paint coats. Whereas the control took ~2 days to reach half saturation, the addition of paint, at minimum, increased this to ~4 days. Most other paints had even larger increases in half saturation time; most between a 3 – 11 fold increase in time.

The increase in $T_{1/2}$ means that the paint acts as a protective vapor barrier that helps keep the wood dry and prevents swelling/damage. Conversely, once the water has been absorbed it takes longer for the water to desorb out; thus paint might promote faster wood decay.

II.6.2 Optimization of ^{14}C -TAZ extraction

As seen in Figure 8, the LLEH protocol was observed to have the same DPM as the controls that had no extraction performed on them. Furthermore, the addition of wood matrix also had no effect on the recovery of ^{14}C -TAZ. Therefore, the LLEH protocol was used for all water samples.

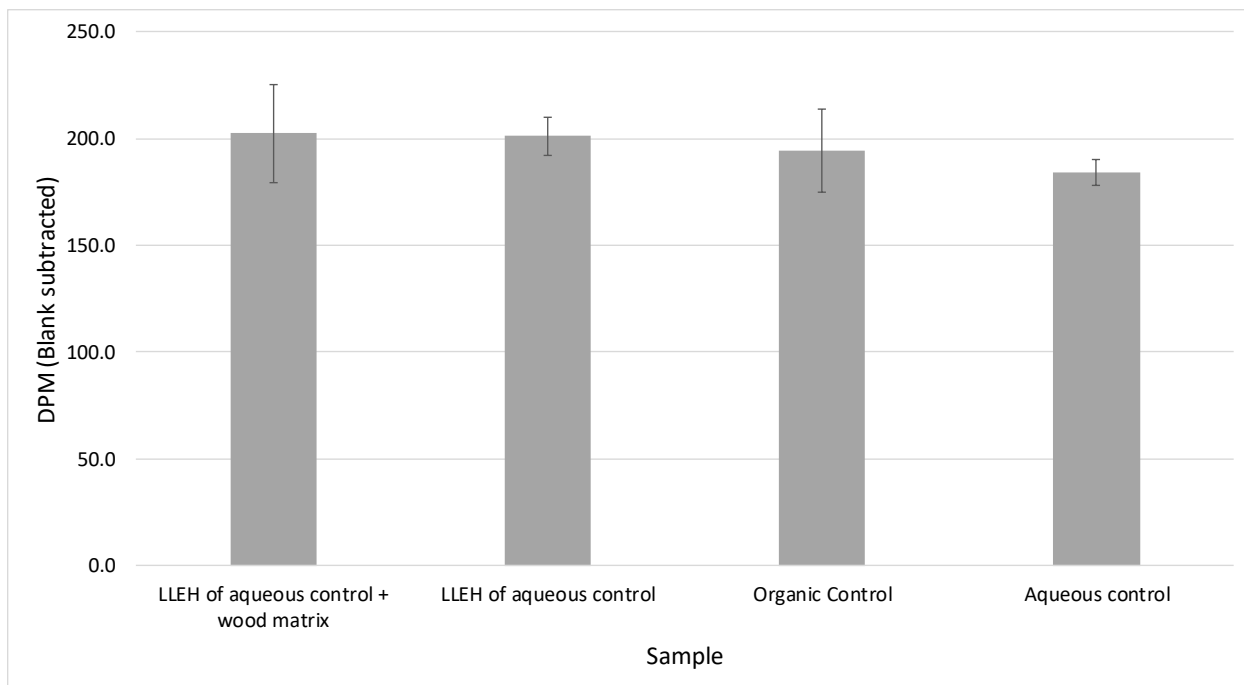


Figure 8. Comparison of extraction techniques on samples.

II.6.3 ^{14}C -TAZ depletion

The amounts of ^{14}C -TAZ recovered from the collected water and acetone are shown in Figure 9. When the amount of wood blocks is factored into the amount of ^{14}C -TAZ collected, there is no statistical difference in the amount collected. Notably, this includes comparing the painted wood to the control (unpainted). Furthermore, the accumulative amount of ^{14}C -TAZ would suggest that the amount being desorbed is removed at a rate significantly slower when compared to samples that were exposed directly to liquid water.

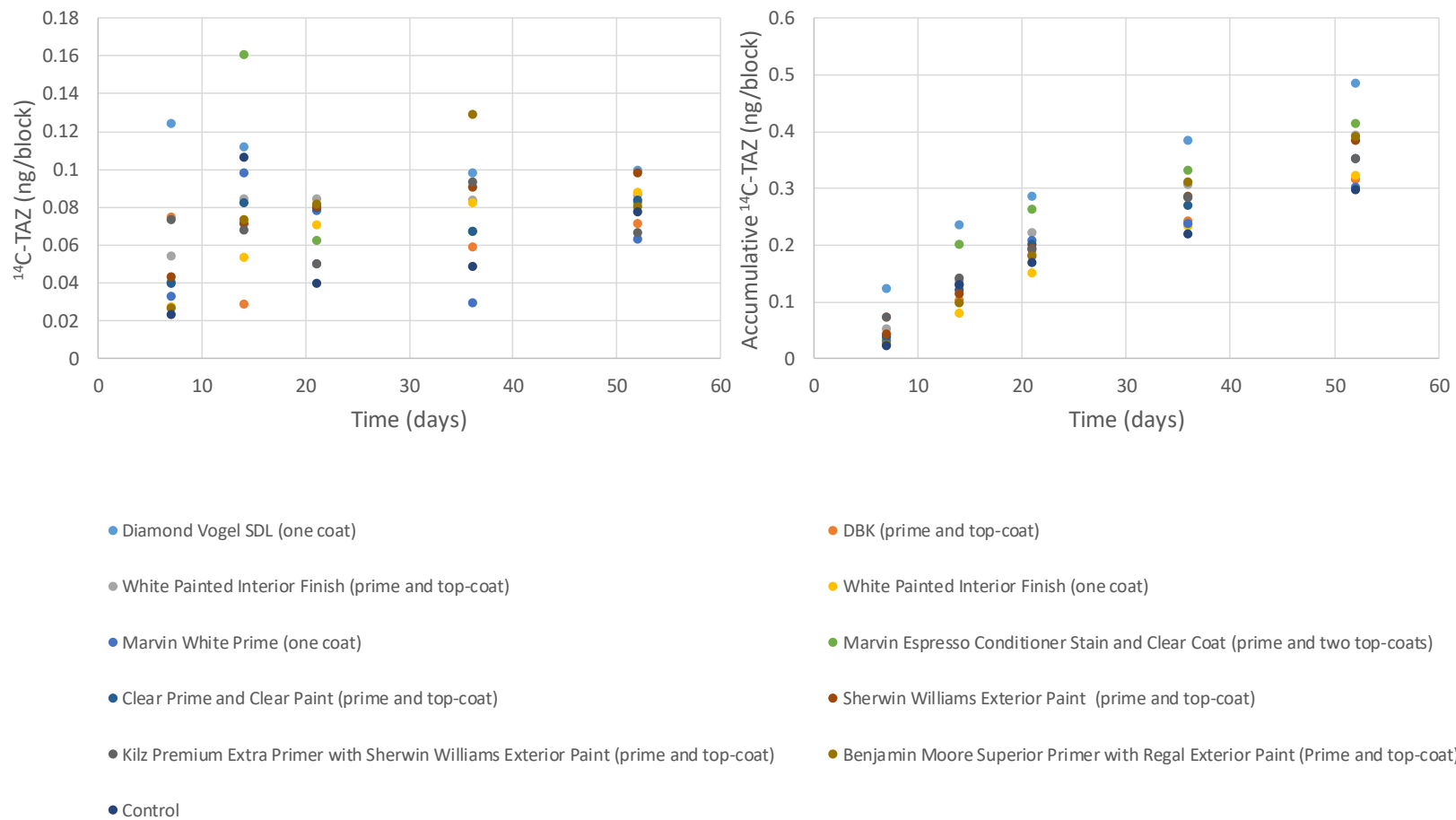


Figure 9. Sum of water and acetone ¹⁴C-TAZ washes. Left display shows individual measurements. Right side display accumulative.

The total amount of ^{14}C -TAZ collected in our previous study on the effect of simulating rain, on both painted and unpainted wood, and the leaching of ^{14}C -TAZ was evaluated for comparison.²¹ After the first two days of simulating rain (flow rate of $\sim 0.1 \text{ mL min}^{-1}$) the amount found in the collected water was three orders of magnitude higher after two days when compared to the amount collected from water vapor after 52 days. Furthermore, the total average amount collected from each block in the current study was less than 0.37 ng ($\sim 650,000,000,000$ atoms). Therefore, the amount of ^{14}C -TAZ desorbed from water vapor should be considered negligible.

II.6.4 Diffusion coefficients comparison

As previously mentioned, diffusion coefficients can be calculated from both the Fickian and empirical equations (Figure 10 below). Both models produce similar values at each time step that the coefficients were solved for. However, the Fickian model produces a more erratic picture of what is happening; often deviating from ideal model diffusion. Conversely, the empirical model appears to “smooth” out these deviations; resulting in diffusion coefficients that do resemble ideal model diffusion. Furthermore, the empirical model can also calculate the diffusion coefficients at any time without a direct measurement as long as $\tau_{1/2}$ is known. This makes it possible to correct for data points that are missing, such as the control beginning and end in this study.

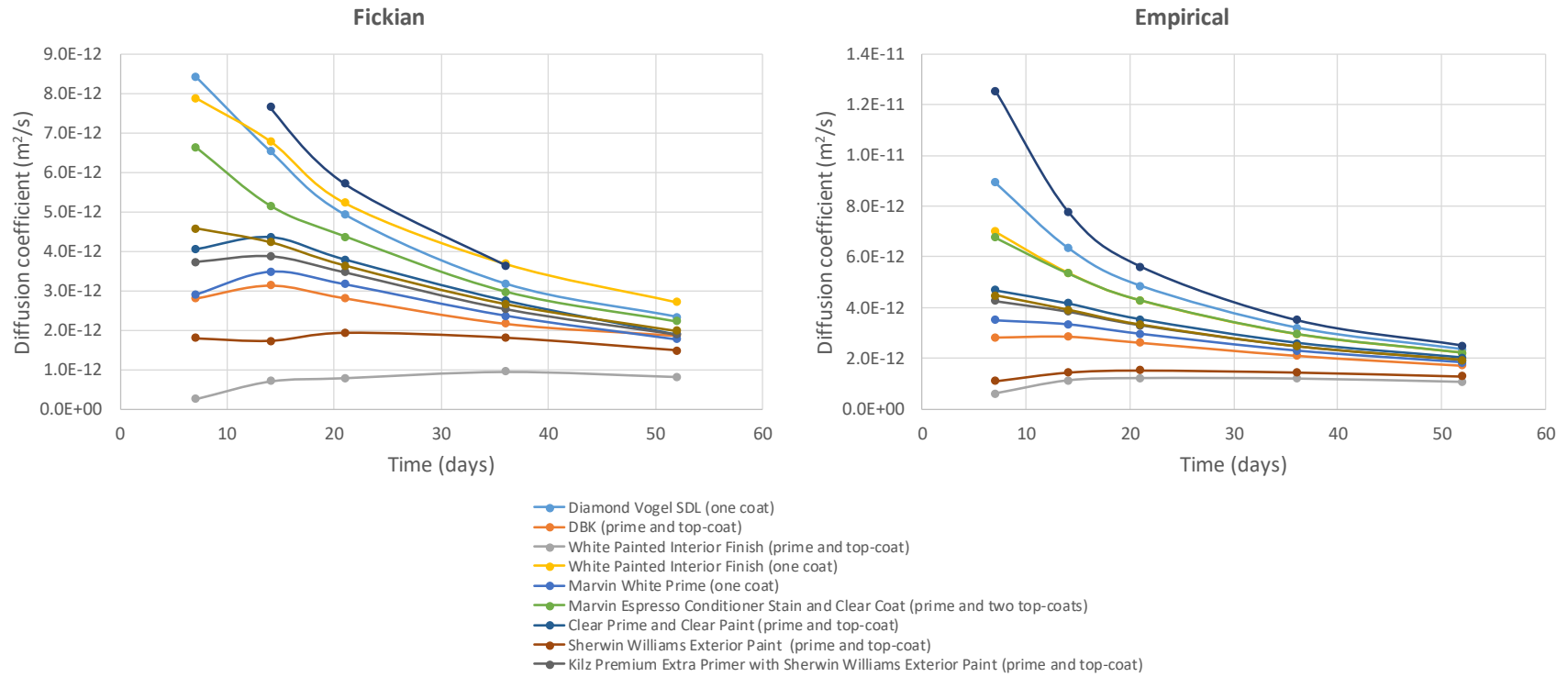


Figure 10. Comparison of solved diffusion coefficients for both Fickian and Empirical models.

II.6.5 Comparison of different wood batches separated by time

Due to the high standard deviation and $\tau_{1/2}$ values observed from White Painted Interior Finish (prime and top-coat), a duplicate study was performed from the same cut of wood several months later. The same paint and primer were applied by Marvin Windows & Doors and a second set of control blocks were used (Figure 11). The results of this duplicate study are inconclusive.

In all cases, the values for H_2O_{max} and $\tau_{1/2}$ were statistically different from each other. In the case of the control, both H_2O_{max} and $\tau_{1/2}$ increased to nearly double. Furthermore, it surpassed the H_2O_{max} of the painted sample; the first instance of a non-painted sample to do so including the old samples. For the White Painted Interior Finish (prime and top-coat), both the $\tau_{1/2}$ value and the standard deviation calculated were reduced significantly.

A possible explanation for the significant variance could be from the difference in initial starting conditions. The University of North Dakota's chemistry labs do not have constant humidity control due to the high air exchange rate needed for its hood system. With the two batches starting months apart (in different seasons) the initial starting humidity would be significantly different. Therefore, future experiments involving this kind of work should conduct everything in close time proximity if a comparison is desired.

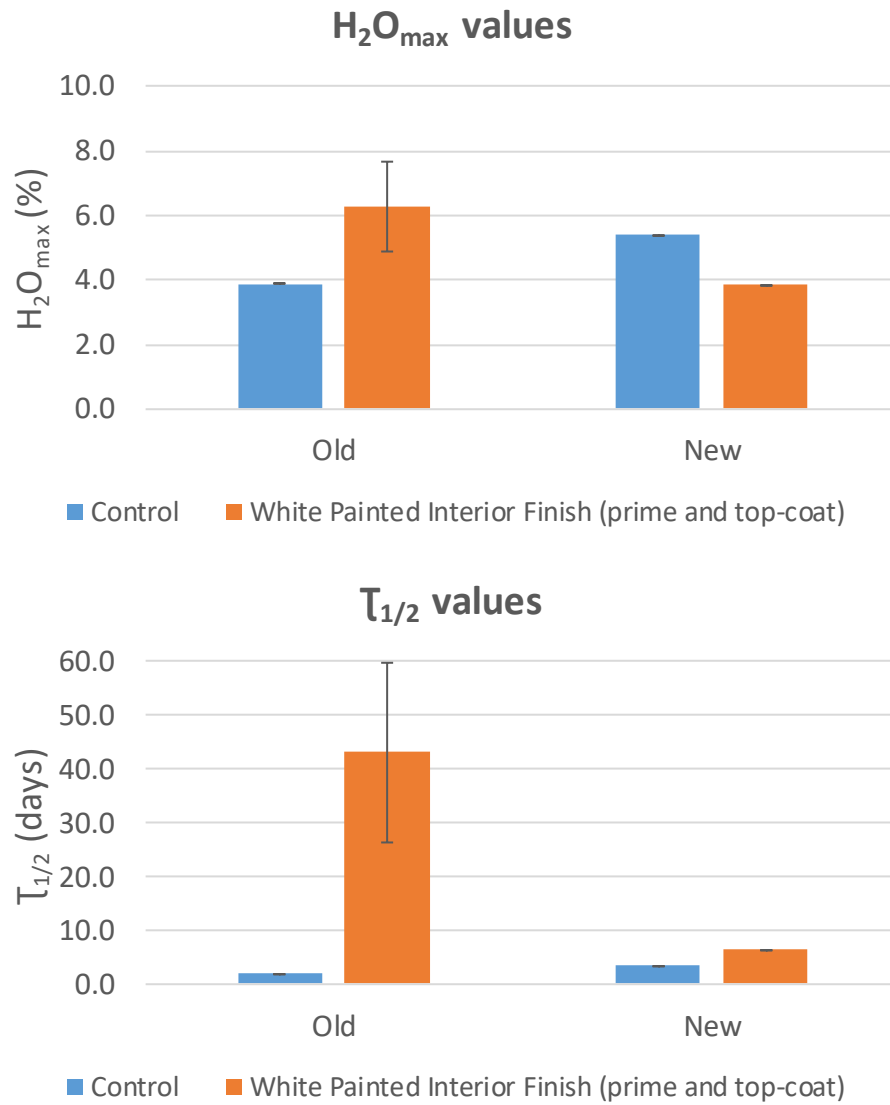


Figure 11. Comparison of old and new samples.

II.6.6 Comparison to double reciprocal calculations

As mentioned previously, double reciprocal plots have been used classically to solve sigmoidal data. Figure 12 illustrates a double reciprocal plot for Clear Prime and Clear Paint (prime and top-coat). Nonlinear regression described this sample, as well as all paint samples, as having

one step of diffusion (further discussed in Chapter III). The double reciprocal plot, however, appears to have two steps or possibly a nonlinear step. Furthermore, double reciprocal calculations over-estimate both H_2O_{max} and $\tau_{1/2}$ while having worse standard deviations for H_2O_{max} (Table 3).

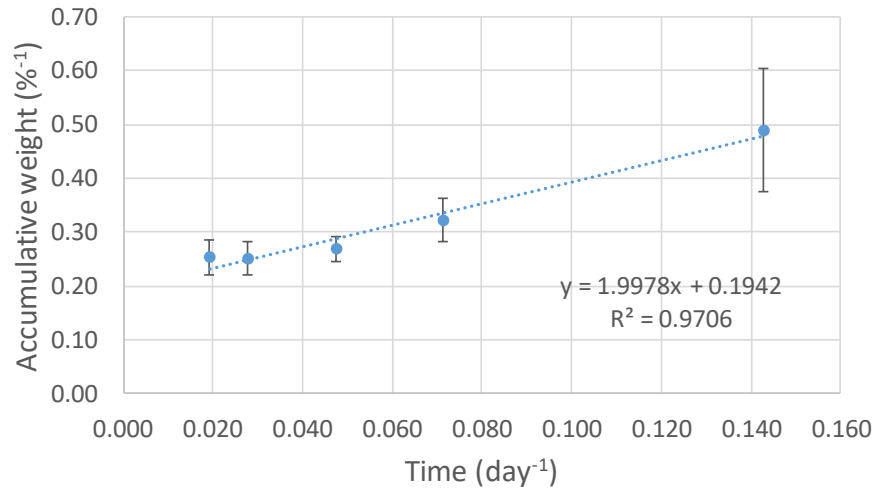


Figure 12. Double reciprocal plot of Clear Prime and Clear Paint (prime and top-coat).

Table 3. Comparison of nonlinear regression and double reciprocal calculations.

Method	H_2O_{max} (%)	$\tau_{1/2}$ (days)
Clear Prime and Clear Paint (prime and top-coat) Nonlinear regression	4.8 ± 0.29	7.8 ± 1.76
Clear Prime and Clear Paint (prime and top-coat) Double reciprocal	5.1 ± 1.8	10.0 ± 1.79

II.7 Conclusion

Painting wood affects both the maximum amount of water vapor it can absorb and the rate at which water vapor is absorbed. For every painted sample tested, the amount of maximum water increased compared to the unpainted sample. Whether the water was inside the wood or absorbed by the paint itself was undetermined. The rate of saturation varied greatly between paint coatings,

but most saw a several fold increase in saturation time. The rate of ^{14}C -TAZ depletion via water vapor was unaffected by paint coating and insignificant overall when compared to direct water exposure.

The empirical model fit well with water vapor absorption measurements, replicating results found with the Fickian model for diffusion coefficients. Moreover, the empirical model was able to “smooth” out deviations from ideal model diffusion observed in the Fickian model and made it possible to find coefficients for missing data points.

CHAPTER III. GRAVIMETRIC ANALYSIS OF LIQUID WATER ABSORPTION

The previous study demonstrated the ability for the empirical model to be used for specifically water vapor absorption in wood (and to a greater extent how paint affected that absorption). To further explore the applications of the model, its use in modeling liquid water absorption was tested and what types of variables change H_2O_{\max} and $T_{1/2}$. Density and water temperature were both evaluated using a full factorial design to understand all interactions that they might have on H_2O_{\max} and $T_{1/2}$.

III.1 Materials

Ponderosa pine sapwood blocks (4 in x 1 in x 0.5 in) were separated into two distinct groups based on density (high 0.430 ± 0.0065 & low 0.335 ± 0.0057 g/cm³). All water used was deionized water from a Direct-Q 3 UV system purifier (Millipore, Billerica, MA, USA).

III.2 Exposure conditions

Each wood block was submerged completely in water to a minimum depth of 2 cm below the surface at either 20 or 40 °C, respectively. At regular intervals the sample was removed from the water, dried with a lint free wipe, weighed, and then returned to the water for a total submerged time of ten minutes.

III.3 Full factorial design

A full factorial 2-factor 2-level design was generated using Minitab 18 (Table 4). Using a full factorial design allowed for any primary and two-way interaction effects to be evaluated.

Table 4. Full factorial design.

StdOrder	RunOrder	CenterPt	Blocks	Density (g/cm ³)	Temperature (°C)
5	1	1	1	0.335	20
1	2	1	1	0.335	20
9	3	1	1	0.335	20
10	4	1	1	0.430	20
2	5	1	1	0.430	20
6	6	1	1	0.430	20
11	7	1	1	0.335	40
7	8	1	1	0.335	40
3	9	1	1	0.335	40
8	10	1	1	0.430	40
4	11	1	1	0.430	40
12	12	1	1	0.430	40

III.4 Nonlinear regression calculations of $\tau_{1/2}$ and H_2O_{max}

Nonlinear regression was used to calculate the values of both $\tau_{1/2}$ and H_2O_{max} in Minitab 18 using Eq. 5. Starting parameters of 1 were used for each constant and a lower bound of greater than zero were used for both. The averaged wood saturation plots can be seen in Appendix F – Averaged saturation plots.

III.5 Statistical analysis

Fractional regression was used to evaluate both responses and their interactions from the factors. Furthermore, a general linear model and one-way ANOVA were used to evaluate H_2O_{max} and $\tau_{1/2}$, respectively, and can be seen in Appendix C & E.

III.6. Results and discussion

The raw results of the nonlinear regression for each sample of wood can be seen in Table 5. Additionally, the plotted accumulative data is shown in Figure 13.

Table 5. Raw results of nonlinear regression calculations.

StdOrder	RunOrder	CenterPt	Blocks	Density (g/cm ³)	Temperature (°C)	H ₂ O _{max} (%)	τ _{1/2} (min)
5	1	1	1	0.335	20	12.17	0.65
1	2	1	1	0.335	20	11.66	1.13
9	3	1	1	0.335	20	12.67	0.66
10	4	1	1	0.430	20	12.79	0.82
2	5	1	1	0.430	20	14.05	0.80
6	6	1	1	0.430	20	13.29	0.78
11	7	1	1	0.335	40	11.67	2.08
7	8	1	1	0.335	40	10.37	1.81
3	9	1	1	0.335	40	11.68	1.35
8	10	1	1	0.430	40	12.46	1.20
4	11	1	1	0.430	40	12.11	1.55
12	12	1	1	0.430	40	13.14	1.78

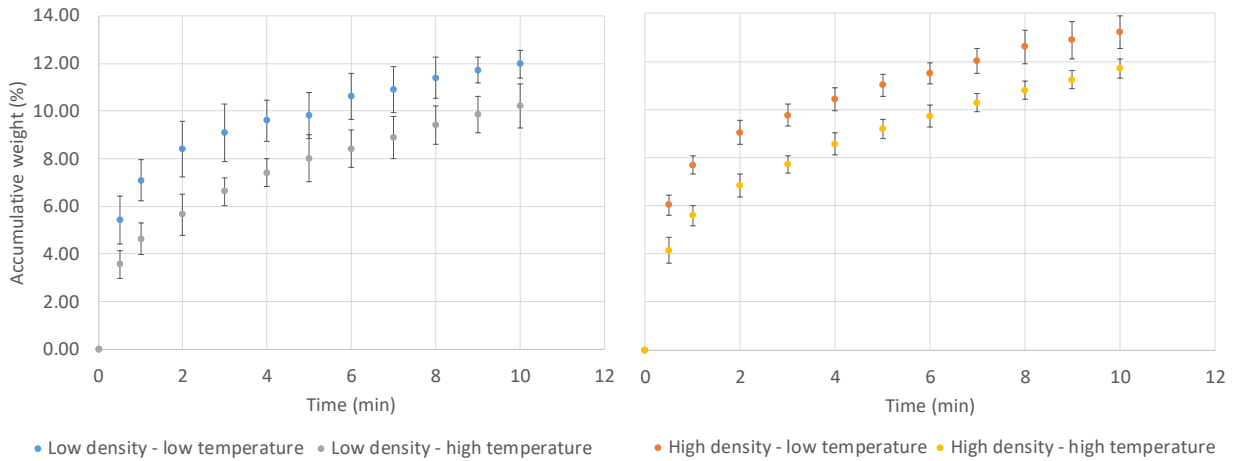


Figure 13. Accumulative weight versus time. Left, low density & right, high density. Error bars are one standard deviation.

III.6.1 H₂O_{max} factors

Analysis of the normal plot (Figure 14) determined that both of the main effects, density and temperature, have an impact on the H₂O_{max} of wood. However, the two-way effect of density*temperature was not significant. Removing the two-way interaction, the results of analysis of variance are presented in Table 6. The normal probability plot, versus fits, and main effects can also be seen in Figure 14. Based on the main effects plot, a higher density and lower temperatures both increase the H₂O_{max}. This result corroborates the trends observed in EMC.³

Table 6. Analysis of variance for H₂O_{max} versus density and temperature.

Source	DF	Adj SS	Adj MS	F-Value	P-Value
Model	2	7.0605	3.53023	10.57	0.004
Linear	2	7.0605	3.53023	10.57	0.004
Density	1	4.8173	4.81726	14.42	0.004
Temperature	1	2.2432	2.2432	6.71	0.029
Error	9	3.0069	0.3341		
Lack-of-Fit	1	0.0113	0.01129	0.03	0.866
Pure Error	8	2.9956	0.37445		
Total	11	10.0673			

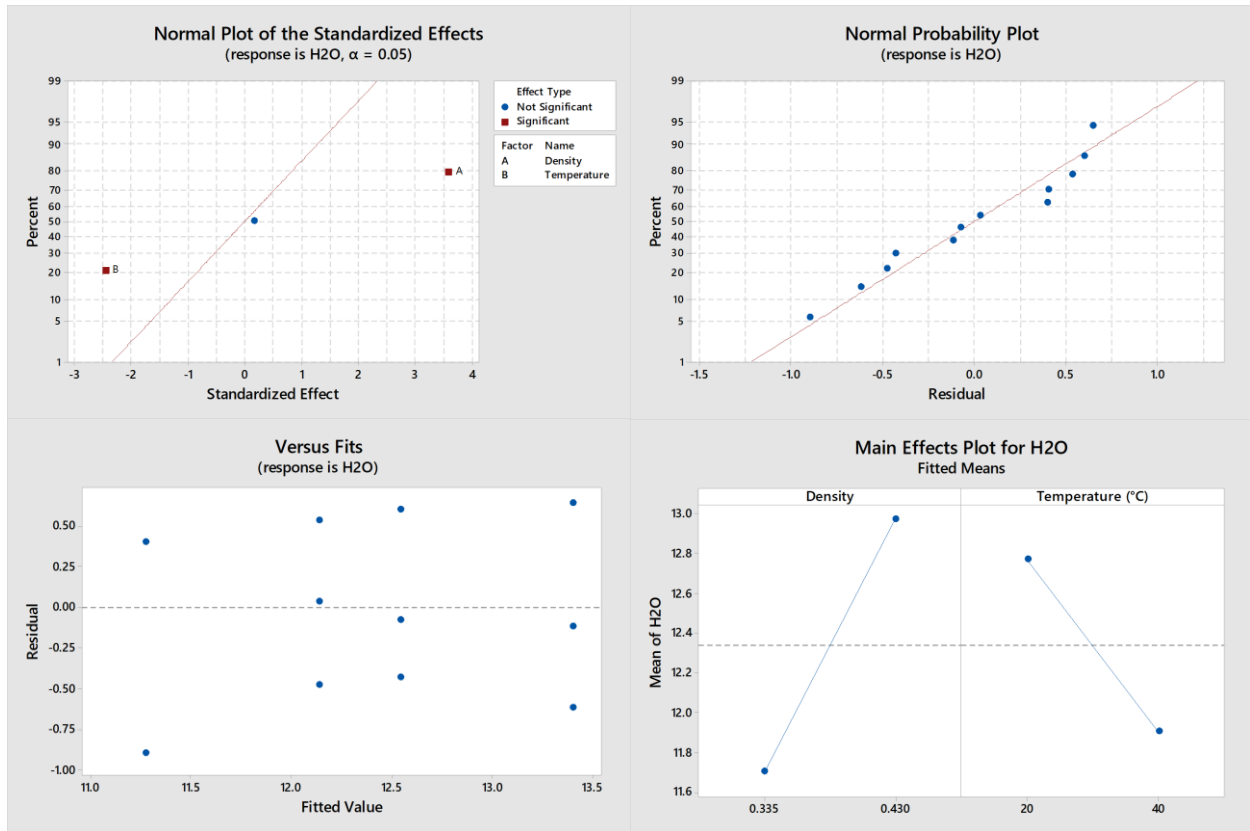


Figure 14. Normal plot, normal probability plot, versus fits, and main effects plots for H₂O_{max}.

III.6.2 $\tau_{1/2}$ factors

Analysis of the normal plot (Figure 15) determined that the only main effect observed was the temperature of water. The results of a reduced model analysis of variance can be seen in Table 7. The normal probability plot, versus fits, and interval plot can also be seen in Figure 15. Based on the interval plot, a higher temperature increases the $\tau_{1/2}$. Increasing the temperature from 20 °C to 40 °C doubled the amount of time needed to obtain half saturation; from 0.81 to 1.63 minutes. Future research should explore this changing $\tau_{1/2}$ with temperature. This phenomena of decreased rate of absorption with higher temperature has not been described in literature. Furthermore, the

rate of absorption is rarely described in most absorption experiments; with most focusing on the maximum amount able to be absorbed.^{25,26}

Table 7. Analysis of variance for $T_{1/2}$ versus temperature.

Source	DF	Adj SS	Adj MS	F-Value	P-Value
Model	1	2.02024	2.02024	29.57	0.000
Linear	1	2.02024	2.02024	29.57	0.000
Temperature	1	2.02024	2.02024	29.57	0.000
Error	10	0.68331	0.06833		
Lack-of-Fit	2	0.08516	0.04258	0.57	0.587
Pure Error	8	0.59814	0.07477		
Total	11	2.70354			

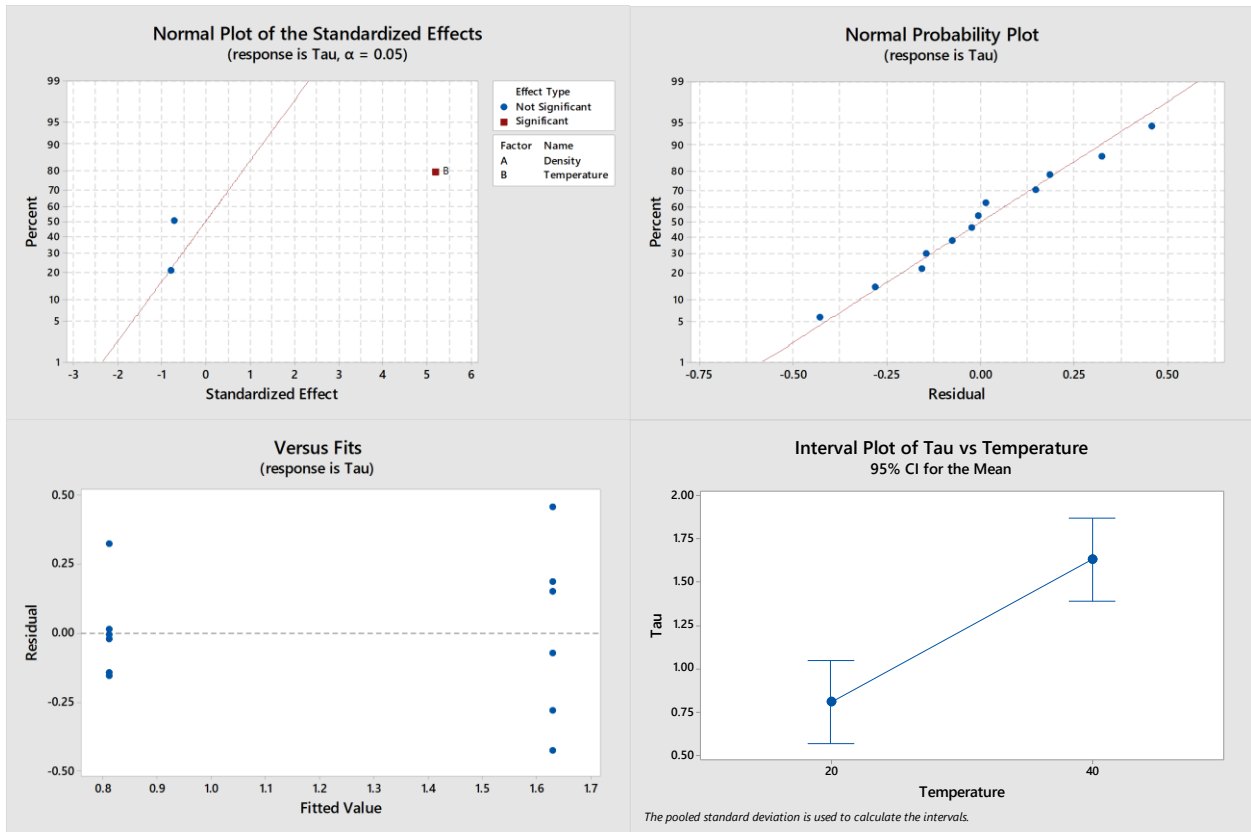


Figure 15. Normal plot, normal probability plot, versus fits, and interval plot plots for $T_{1/2}$.

III.6.3 Multiple steps of diffusion

The previous two sections describe the effects on H_2O_{max} and $T_{1/2}$ when each sample was analyzed independently, which is beneficial to understanding their impact. However, when analyzing the samples in their groups other trends were observed; specifically, two steps of diffusion with the high-density wood. All averaged results can be seen in Appendix D.

High-density wood exposed to both high and low temperature showed multiple steps of diffusion. This was concluded based on the “Lack of Fit” error expressed in the nonlinear regression statistics, which had a P value of 0. Thus, the model was incapable of being applied to the data recorded. However, by systematically “trimming off” data from the longer times to shorter the Lack of Fit error P value increased till it was greater than 0.05. Consequently, the model was then applicable to both sets of data (untrimmed and trimmed) as seen in Table 8.

Table 8. H_2O_{max} and $T_{1/2}$ averaged values for all conditions. No standard deviations were greater than 10^{-5} for H_2O_{max} and were consequently omitted.

Factor	H_2O_{max} (%)	$T_{1/2}$ (minutes)
Low density - low temperature	12.17	0.90 ± 0.060
Low density - high temperature	10.56	1.75 ± 0.060
High density - low temperature 0-5 minutes	11.67	0.51 ± 0.023
High density - low temperature 6-10 minutes	17.35	3.16 ± 0.035
High density - high temperature 0-6 minutes	10.74	0.95 ± 0.042
High density - high temperature 7-10 minutes	17.13	4.68 ± 0.013

With the separation of first and second step diffusion in the high-density wood, several new observations come out. The H_2O_{max} for each high-density first step is similar to its respective temperature low-density H_2O_{max} . Furthermore, the H_2O_{max} for high density, second step diffusion is also similar in value. $T_{1/2}$ still follows the trend described in previously, with lower temperatures

having faster rates of half saturation. It can also be noted that the second step diffusion $\tau_{1/2}$ is several orders of magnitude higher than the first step.

III.6.4 Comparison to double reciprocal calculation

To further demonstrate the advantage of using nonlinear regression, a double reciprocal plot was made for the samples that were high density and low temperature (Figure 16). The H_2O_{max} and $\tau_{1/2}$ values were based on the times discovered via nonlinear regression. Therefore, this should be treated as an optimal data calculation, because double reciprocal plots have no indication of when to parse the data.

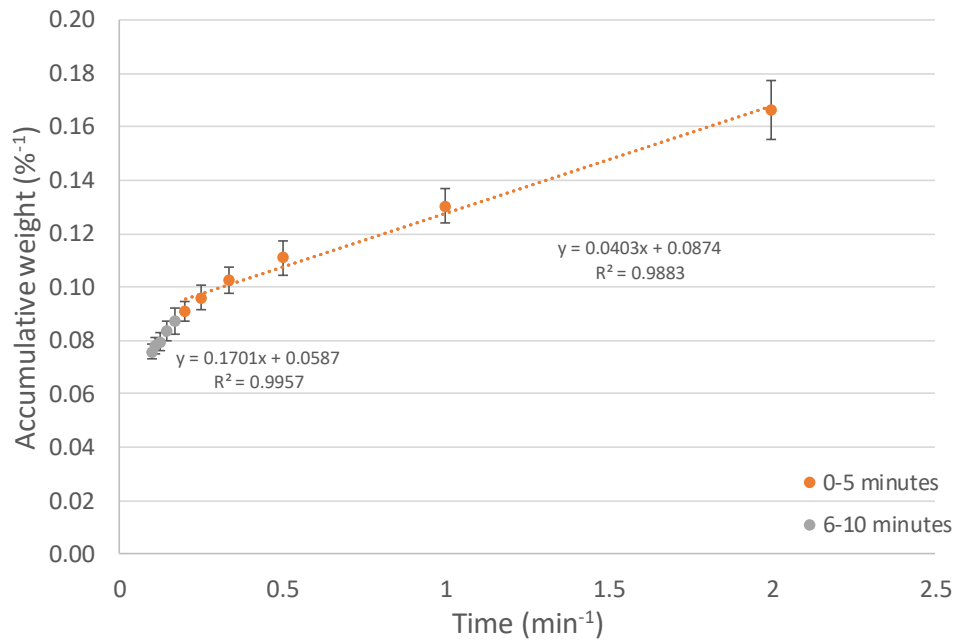


Figure 16. Double reciprocal plot of High density - low temperature.

Table 9. Comparison of H_2O_{max} and $T_{1/2}$ via nonlinear regression and double reciprocal calculations. Standard deviation for H_2O_{max} nonlinear regression was greater than 10^{-5} and was consequently omitted.

Method	H_2O_{max} (%)	$T_{1/2}$ (minutes)
High density - low temperature 0-5 minutes Nonlinear regression	11.67	0.51 ± 0.023
High density - low temperature 6-10 minutes Nonlinear regression	17.35	3.16 ± 0.035
High density - low temperature 0-5 minutes Double reciprocal	11.4 ± 0.62	0.46 ± 0.027
High density - low temperature 6-10 minutes Double reciprocal	17.0 ± 0.65	2.9 ± 0.12

As seen in Table 9, the values for H_2O_{max} are similar for both methods in step of diffusion. However, the standard deviation between the two is significantly different. Nonlinear regression calculates the standard deviation being around 10^{-5} , while double reciprocal calculations are at 10^{-1} . As for $T_{1/2}$, double reciprocal underestimates the values and has a significant different standard deviation for the second step of diffusion.

III.7. Conclusion

Liquid water diffusion was able to be analyzed by the empirical model; further expanding its application. Furthermore, the effect of density and temperature were analyzed for H_2O_{max} and $T_{1/2}$. The maximum amount of water that ponderosa pine sapwood can absorb is influenced by the initial density and the temperature of the water it is submerged in. A higher density and lower water temperature were observed to raise the amount of water absorbed. The amount of time to reach half saturation was only influenced by temperature; in which, higher temperatures lead to longer half saturation times.

Two steps of diffusion were observed in high density wood at both temperatures. The values of H_2O_{max} and $T_{1/2}$ for each step was calculated using nonlinear regression, which showed that the first step of diffusion was similar to that of the low-density wood with respect to

temperature. The two steps of diffusion were also analyzed via double reciprocal plots, which demonstrated the inefficacy of double reciprocal plots even when using the best parsing based on nonlinear regression calculations.

CHAPTER IV. ABSORPTION OF VARIOUS SOLVENTS INTO A WOOD MATRIX

As shown in the previous two chapters, both liquid water and water vapor diffuse (absorb) into wood in predictable ways that are described previously by Eq. 5. To further investigate the applicability of this empirical model, several different solvents were tested.

IV.1 Materials

n-Hexadecane was purchased from Alfa Aesar (Ward Hill, Massachusetts). Woodlife 111 RTU was purchased from Kop-Coat, Inc. (Pittsburgh, Pennsylvania) and is characterized as a nonpolar solvent with 0.22% dissolved fungicides for treating wood. Ponderosa pine (3.8 cm x 3.9 cm x 15 cm) was used for submersion in distilled water, *n*-hexadecane, and Woodlife.

IV.2 Exposure conditions

Each block of wood was partially submerged ~1 cm vertically in a glass container in the appropriate solvent. Diffusion takes place significantly in the transversal via capillary action; therefore, with only one end submerged, these values should be considered an underestimate of the total amount that can be absorbed. The solvent was maintained at the same height with periodic refills of solvent. Before each gravimetric measurement, the wood block was wiped with a lint-free tissue to remove excess solvent. After being weighed, it was returned to the solvent. All containers were sealed between measurements to prevent solvent loss. The *n*-Hexadecane and water data was recorded by Ganna Baglayeva and originally published in Forest Products Journal (DOI: 10.13073/FPJ-D-15-00086). The Woodlife 111 RTU data was recorded by Klara Kukowski and originally published in International Journal of Heat and Mass Transfer (DOI: 10.1016/j.ijheatmasstransfer.016.06.097).^{4,11}

IV.3 Estimation of maximum solvent uptake and half saturation time

The empirical equation from Eq. 5 was used with nonlinear regression to solve for $\text{Solvent}_{\text{max}}$ and $\tau_{1/2}$.

IV.4 Results and discussion

Non-linear regression incorporating the empirical model was applied to each solvent tested and the results for $\text{Solvent}_{\text{max}}$ and $\tau_{1/2}$ are shown in Table 10 and individual results can be found in Appendix G.

Water had both the highest amount absorbed and the longest saturation time when compared to the other (non-polar) solvents; absorbing twice as much as *n*-hexadecane and nearly four times as much as Woodlife, while taking twice and 61 times longer to absorb it, respectively (Figure 17). *n*-Hexadecane and Woodlife are both nonpolar but have significantly different values of $\tau_{1/2}$. While Woodlife is a proprietary and its makeup is not public information, the safety data sheet refers the solvent as 98% volatile organic compounds (VOCs) with a flash point of 40 °C. In comparison, *n*-hexadecane has a flash point of 135 °C. This would suggest that Woodlife is made of lower molecular weight solvents which could give insight into why $\tau_{1/2}$ is faster. Conversely, with having smaller molecules, it would be expected that it would have a higher $\text{Solvent}_{\text{max}}$, but that is not observed. Furthermore, Woodlife is a mixture of different solvents and additives, which may have competing absorptions that are not disruptive to the model but still lower the overall $\text{Solvent}_{\text{max}}$. Lastly, the mechanism of absorption for non-water solvents should be inherently different. However, this is beyond the scope of this work and was not investigated.

Table 10. Results of nonlinear regression.

	Water	<i>n</i> -Hexadecane	Woodlife
Solvent_{max} (%)	14.2 ± 0.58	6.05776 ± 0.00073	3.476 ± 0.0033
T_{1/2} (min)	55 ± 7.7	13.638600 ± 0.0000036	0.90 ± 0.066

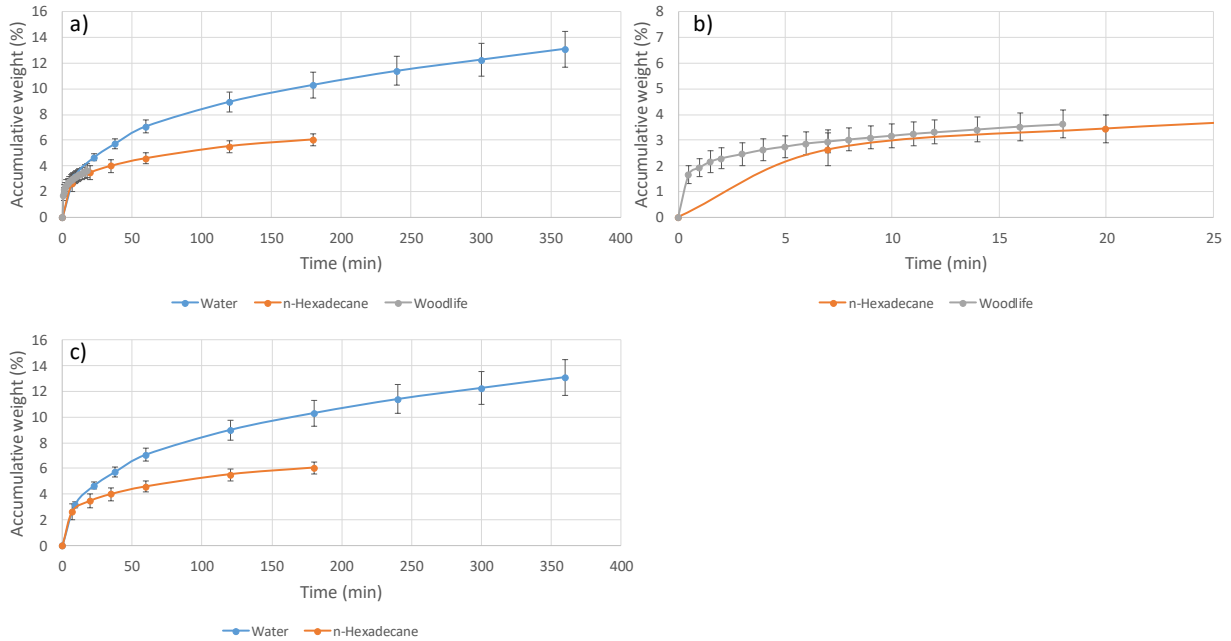


Figure 17. Saturation graphs of water, *n*-hexadecane, and Woodlife. a) Comparison of all three. b) Zoomed in section comparing *n*-Hexadecane and Woodlife. c) Comparison of water and *n*-hexadecane.

IV.5 Conclusion

The empirical model was successfully applied to water and two nonpolar solvents which demonstrated its applicability to more than water; as demonstrated in previous chapters. Water was observed having higher amounts absorbed while also having slower saturation rates when compared to the two nonpolar solvents.

CHAPTER V. CONCLUSIONS

The summation of the previous chapters can be categorized into two main topics: the results of the wood absorption for various conditions and the model's applicability to each system. The various conditions evaluated were: the measurement of water vapor absorption and how paint affected the H_2O_{max} and $T_{1/2}$ as well as the possible leaching of ^{14}C -TAZ, liquid water absorption and how the density of the wood and temperature of the water affected H_2O_{max} and $T_{1/2}$, and the potential validity of applying the empirical model to organic solvents in wood absorption.

Painting wood affected both the maximum amount of water vapor it can absorb and the rate at which water vapor is absorbed. For every painted sample tested, the amount of maximum water increased compared to the unpainted sample. The rate of saturation varied greatly between paint coatings, but most saw a several fold increase in saturation time.

There is no statistical difference between the painted wood and unpainted wood in regards to the rate at which ^{14}C -TAZ leaches. Furthermore, the amount leached is nearly nothing when compared to the amount lost from simulated rain. The average total amount collected was less than 0.37 ng per wood block after 52 days. The amount from simulated rain was thousands of times above that.²¹

The H_2O_{max} was found to be influenced by both the initial density and the temperature of the water it is submerged in. A higher density and lower water temperature were observed to maximize the amount of water absorbed. Whereas, the $T_{1/2}$ was only influenced by temperature; in which, higher temperatures lead to longer half saturation times.

The empirical model was successfully applied to water and two nonpolar solvents which demonstrated its applicability to more than water; as demonstrated in previous chapters. Water

was observed having higher amounts absorbed while also having slower saturation rates when compared to the two nonpolar solvents.

The applicability of the empirical model was demonstrated with water vapor, liquid water, and organic solvents. In every case, it provided an estimate of estimate of the maximum amount of water absorption; something of which was previously only done via direct experimentation over very long time scales.^{4,11,12,18} Furthermore, $\tau_{1/2}$ demonstrated that it can describe the rate of absorption (what a single diffusion coefficient cannot); while still being able to solve for diffusion coefficients if needed.

APPENDICES

Appendix A – Algebraic proof of solving diffusion coefficients from empirical model

Fick's second law of diffusion

$$\frac{w_t - w_0}{w_\infty - w_0} = \frac{2}{\sqrt{\pi}} \left(\frac{A}{V} \right) \sqrt{Dt}$$

Empirical formula

$$H_2O_{(t)} = H_2O_{(max)} \left(\frac{t}{\tau_{1/2} + t} \right)$$

$$w_t - w_0 = H_2O_{(t)}$$

$$w_\infty - w_0 = H_2O_{(max)}$$

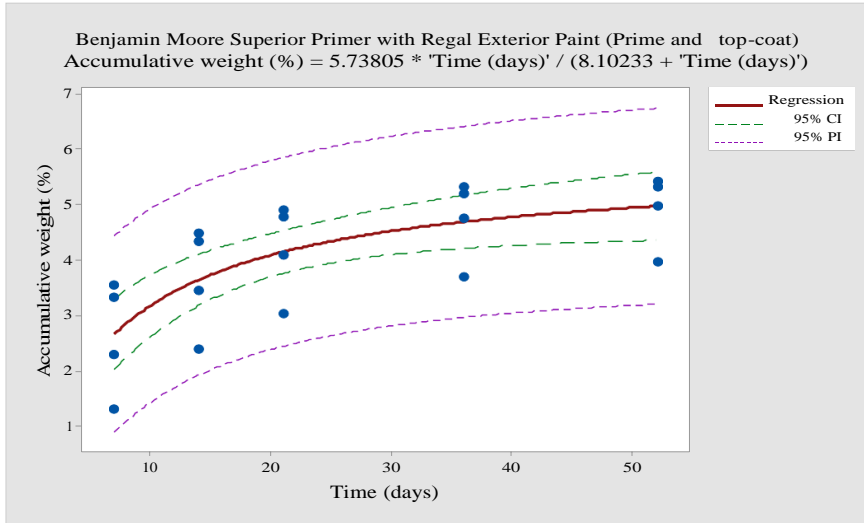
$$\frac{H_2O_{(t)}}{H_2O_{(max)}} = \frac{2}{\sqrt{\pi}} \left(\frac{A}{V} \right) \sqrt{Dt}$$

$$H_2O_{(t)} = \left[\frac{2}{\sqrt{\pi}} \left(\frac{A}{V} \right) \sqrt{Dt} \right] H_2O_{(max)}$$

$$\text{Therefore } \left[\frac{2}{\sqrt{\pi}} \left(\frac{A}{V} \right) \sqrt{Dt} \right] = \left(\frac{t}{\tau_{1/2} + t} \right)$$

$$D = \frac{t\pi V^2}{4(\tau_{1/2} + t)^2 A^2}$$

Appendix B – Individual Minitab for paint results



Nonlinear Regression: Accumulative weight (%) = H2O * ... s' / (T + ...

Method

Gauss-Newton

Algorithm

200

Max iterations

Tolerance

0.00001

Starting Values for Parameters

Parameter

Value

H2O

1

T

1

Constraints on Parameters

0 < H2O

0 < T

Equation

Accumulative weight (%) = 5.73805 * 'Time (days)' / (8.10233 + 'Time (days)')

Parameter Estimates

Parameter

Estimate

SE Estimate

H2O

5.73805

0.0018233

T

8.10233

0.0008819

Accumulative weight (%) = H2O * 'Time (days)' / (T + 'Time (days)')

Lack of Fit

Source

DF

SS

MS

F

P

Error

18

11.1316

0.618421

Lack of Fit

3

0.0426

0.014196

0.02

0.996

Pure Error

15

11.089

0.739266

Summary

Iterations

7

Final SSE

11.1316

DFE

18

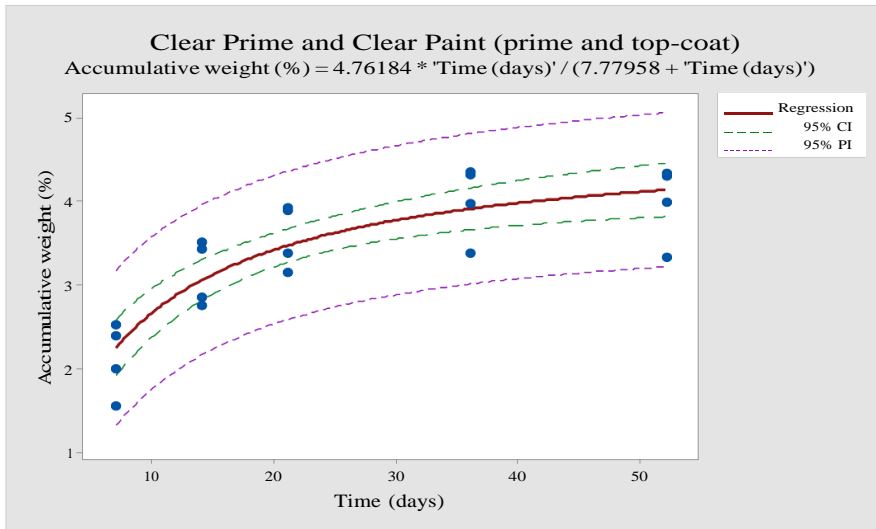
MSE

0.618421

S

0.786398

Fitted Line: Accumulative weight (%) versus Time (days)



Nonlinear Regression: Accumulative weight (%) = H2O * ... s)' / (T + ...

Method

Gauss-Newton

Algorithm

200

Max iterations

Tolerance

0.00001

Starting Values for Parameters

Parameter

Value

H2O

1

T

1

Constraints on Parameters

0 < H2O

0 < T

Equation

Accumulative weight (%) = 4.76184 * 'Time (days)' / (7.77958 + 'Time (days)')

Parameter Estimates

Parameter

Estimate

SE Estimate

H2O

4.76184

0.0024766

T

7.77958

0.0007365

Accumulative weight (%) = H2O * 'Time (days)' / (T + 'Time (days)')

Lack of Fit

Source

DF

SS

MS

F

P

Error

18

3.03807

0.168782

Lack of Fit

3

0.27881

0.092936

0.51

0.685

Pure Error

15

2.75926

0.183951

Summary

Iterations

7

Final SSE

3.03807

DFE

18

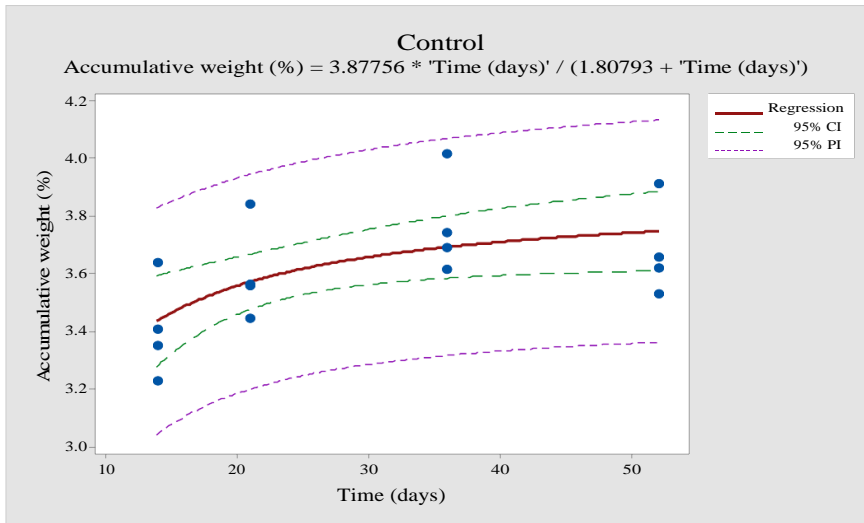
MSE

0.168782

S

0.410831

Fitted Line: Accumulative weight (%) versus Time (days)



Nonlinear Regression: Accumulative weight (%) = $H2O * \dots s' / (T + \dots$

Method	Gauss-Newton
Algorithm	
Max iterations	200
Tolerance	0.00001
Starting Values for Parameters	
Parameter	Value
H2O	1
T	1

Constraints on Parameters

$0 < H2O$

$0 < T$

Equation

Accumulative weight (%) = $3.87756 * \text{'Time (days)'} / (1.80793 + \text{'Time (days)'})$

Parameter Estimates

Parameter	Estimate	SE Estimate
H2O	3.87756	0.002237
T	1.80793	0.112535

Accumulative weight (%) = $H2O * \text{'Time (days)'} / (T + \text{'Time (days)'})$

Lack of Fit

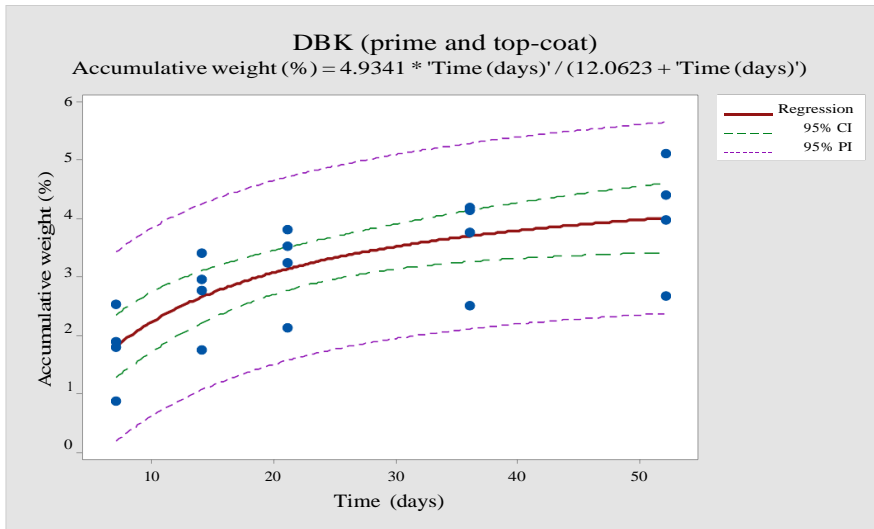
Source

	DF	SS	MS	F	P
Error	14	0.39576	0.0282686		
Lack of Fit	2	0.04742	0.0237099	0.82	0.465
Pure Error	12	0.348341	0.0290284		

Summary

Iterations	7
Final SSE	0.39576
DFE	14
MSE	0.0282686
S	0.168133

Fitted Line: Accumulative weight (%) versus Time (days)



Nonlinear Regression: Accumulative weight (%) = H2O * ... s' / (T + ...

Method

Gauss-Newton

Algorithm

200

Max iterations

0.00001

Tolerance

Starting Values for Parameters

Parameter

Value

H2O

1

T

1

Constraints on Parameters

0 < H2O

0 < T

Equation

Accumulative weight (%) = 4.9341 * 'Time (days)' / (12.0623 + 'Time (days)')

Parameter Estimates

Parameter

Estimate

SE Estimate

H2O

4.9341

0.0047434

T

12.0623

0.0000279

Accumulative weight (%) = H2O * 'Time (days)' / (T + 'Time (days)')

Lack of Fit

Source

DF

SS

MS

F

P

Error

18

9.45664

0.525369

Lack of Fit

3

0.04103

0.013676

0.02

0.995

Pure Error

15

9.41561

0.627708

Summary

Iterations

6

Final SSE

9.45664

DFE

18

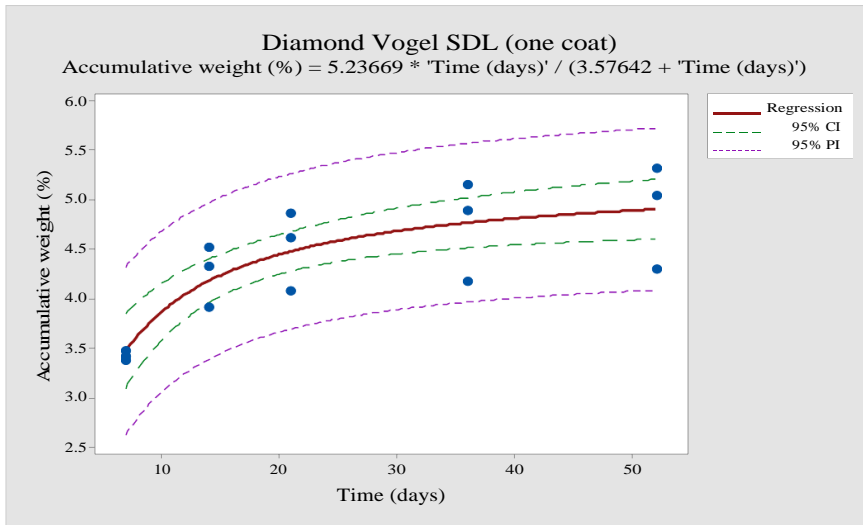
MSE

0.525369

S

0.724823

Fitted Line: Accumulative weight (%) versus Time (days)



Nonlinear Regression: Accumulative weight (%) = H2O * ... s' / (T + ...

Method

Gauss-Newton

Algorithm

200

Max iterations

Tolerance

0.00001

Starting Values for Parameters

Parameter

Value

H2O

1

T

1

Constraints on Parameters

0 < H2O

0 < T

Equation

Accumulative weight (%) = 5.23669 * 'Time (days)' / (3.57642 + 'Time (days)')

Parameter Estimates

Parameter

Estimate

SE Estimate

H2O

5.23669

0.0011277

T

3.57642

0.0237293

Accumulative weight (%) = H2O * 'Time (days)' / (T + 'Time (days)')

Lack of Fit

Source

DF

SS

MS

F

P

Error

13

1.60407

0.12339

Lack of Fit

3

0.03051

0.01017

0.06

0.977

Pure Error

10

1.57356

0.157356

Summary

Iterations

8

Final SSE

1.60407

DFE

13

MSE

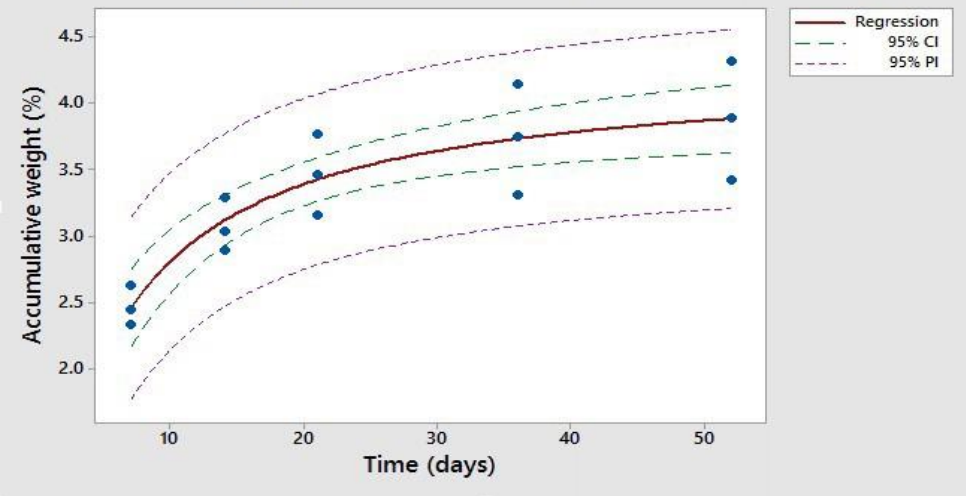
0.12339

S

0.351269

Fitted Line: Accumulative weight (%) versus Time (days)

Marvin Espresso Conditioner Stain and Clear Coat (prime and two top-coats)
Accumulative weight (%) = 4.26294 * 'Time (days)' / (5.18286 + 'Time (days)')



Nonlinear Regression: Accumulative weight (%) = H2O * ... s' / (T + ...

Method

Algorithm

Gauss-Newton

Max iterations

200

Tolerance

0.00001

Starting Values for Parameters

Parameter

Value

H2O

1

T

1

Constraints on Parameters

0 < H2O

0 < T

Equation

Accumulative weight (%) = 4.26294 * 'Time (days)' / (5.18286 + 'Time (days)')

Parameter Estimates

Parameter

Estimate

SE Estimate

H2O

4.26294

0.0027628

T

5.18286

0.0062361

Accumulative weight (%) = H2O * 'Time (days)' / (T + 'Time (days)')

Lack of Fit

Source

DF

SS

MS

F

P

Error

13

1.07711

0.082855

Lack of Fit

3

0.01092

0.00364

0.03

0.991

Pure Error

10

1.06619

0.106619

Summary

Iterations

7

Final SSE

1.07711

DFE

13

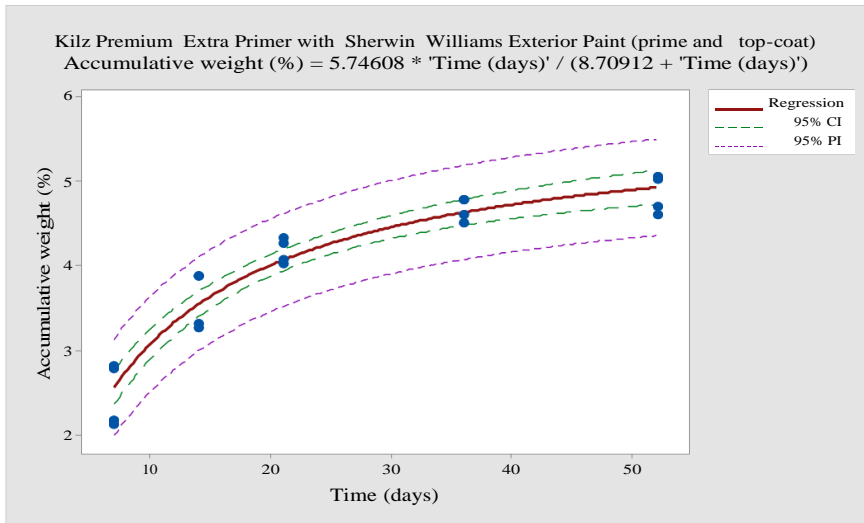
MSE

0.0828546

S

0.287845

Fitted Line: Accumulative weight (%) versus Time (days)



Nonlinear Regression: Accumulative weight (%) = H2O * ... s' / (T + ...

Method

Gauss-Newton

Algorithm

200

Max iterations

0.00001

Tolerance

Starting Values for Parameters

Parameter

Value

H2O

1

T

1

Constraints on Parameters

0 < H2O

0 < T

Equation

Accumulative weight (%) = 5.74608 * 'Time (days)' / (8.70912 + 'Time (days)')

Parameter Estimates

Parameter

Estimate

SE Estimate

H2O

5.74608

0.0006062

T

8.70912

0.0001667

Accumulative weight (%) = H2O * 'Time (days)' / (T + 'Time (days)')

Lack of Fit

Source

DF

SS

MS

F

P

Error

18

1.15847

0.0643595

Lack of Fit

3

0.10828

0.0360929

0.52

0.678

Pure Error

15

1.05019

0.0700128

Summary

Iterations

8

Final SSE

1.15847

DFE

18

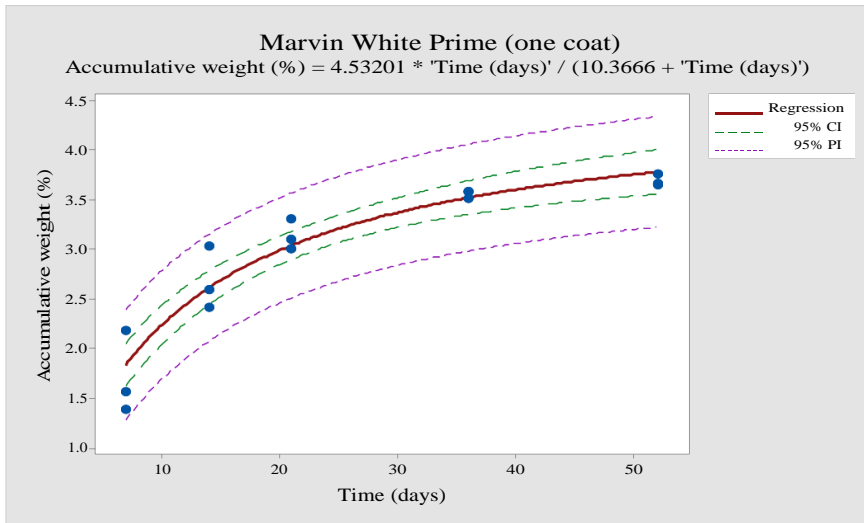
MSE

0.0643595

S

0.253692

Fitted Line: Accumulative weight (%) versus Time (days)



Nonlinear Regression: Accumulative weight (%) = H2O * ... s' / (T + ...

Method

Gauss-Newton

Algorithm

200

Max iterations

0.00001

Tolerance

Starting Values for Parameters

Parameter

Value

H2O

1

T

1

Constraints on Parameters

0 < H2O

0 < T

Equation

Accumulative weight (%) = 4.53201 * 'Time (days)' / (10.3666 + 'Time (days)')

Parameter Estimates

Parameter

Estimate

SE Estimate

H2O

4.532

0.0024251

T

10.3666

0.0000522

Accumulative weight (%) = H2O * 'Time (days)' / (T + 'Time (days)')

Lack of Fit

Source

DF

SS

MS

F

P

Error

13

0.725714

0.0558241

Lack of Fit

3

0.119976

0.0399919

0.66

0.595

Pure Error

10

0.605738

0.0605738

Summary

Iterations

8

Final SSE

0.725714

DFE

13

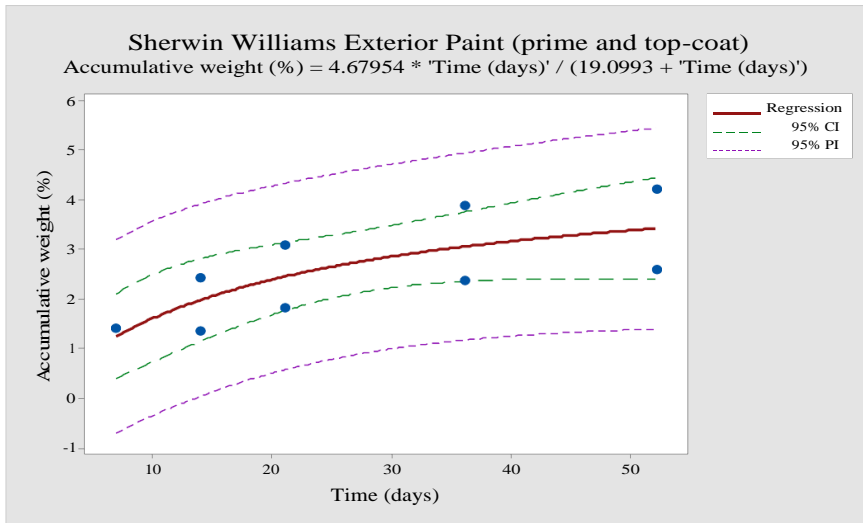
MSE

0.0558241

S

0.236271

Fitted Line: Accumulative weight (%) versus Time (days)



Nonlinear Regression: Accumulative weight (%) = $H2O * \dots s' / (T + \dots$

Method Gauss-Newton
 Algorithm
 Max iterations 200
 Tolerance 0.00001
 Starting Values for Parameters
 Parameter Value
 H2O 1
 T 1

Constraints on Parameters

$0 < H2O$

$0 < T$

Equation

Accumulative weight (%) = $4.67954 * \text{'Time (days)'} / (19.0993 + \text{'Time (days)'})$

Parameter Estimates

Parameter	Estimate	SE Estimate
H2O	4.6795	0.0133425
T	19.0993	0.0000001

Accumulative weight (%) = $H2O * \text{'Time (days)'} / (T + \text{'Time (days)'})$

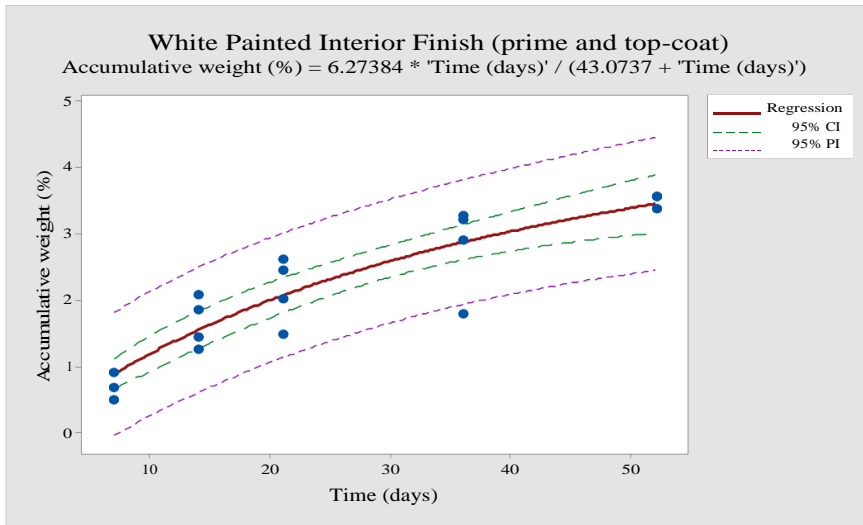
Lack of Fit

Source	DF	SS	MS	F	P
Error	7	3.82463	0.546375		
Lack of Fit	3	0.05193	0.01731	0.02	0.996
Pure Error	4	3.7727	0.943175		

Summary

Iterations	7
Final SSE	3.82463
DFE	7
MSE	0.546375
S	0.739172

Fitted Line: Accumulative weight (%) versus Time (days)



Nonlinear Regression: Accumulative weight (%) = $H2O * \dots s' / (T + \dots$

Method Gauss-Newton
 Algorithm
 Max iterations 200
 Tolerance 0.00001
 Starting Values for Parameters
 Parameter Value
 H2O 1
 T 1

Constraints on Parameters

$0 < H2O$

$0 < T$

Equation

Accumulative weight (%) = $6.27384 * \text{'Time (days)' / (43.0737 + \text{'Time (days)'}$)

Parameter Estimates

Parameter	Estimate	SE Estimate
H2O	6.2738	0.0026234
T	43.0737	0

Accumulative weight (%) = $H2O * \text{'Time (days)' / (T + \text{'Time (days)'}$)

Lack of Fit

Source

	DF	SS	MS	F	P
Error	16	2.86212	0.178882		
Lack of Fit	3	0.20115	0.067049	0.33	0.806
Pure Error	13	2.66097	0.20469		

Summary

Iterations 8

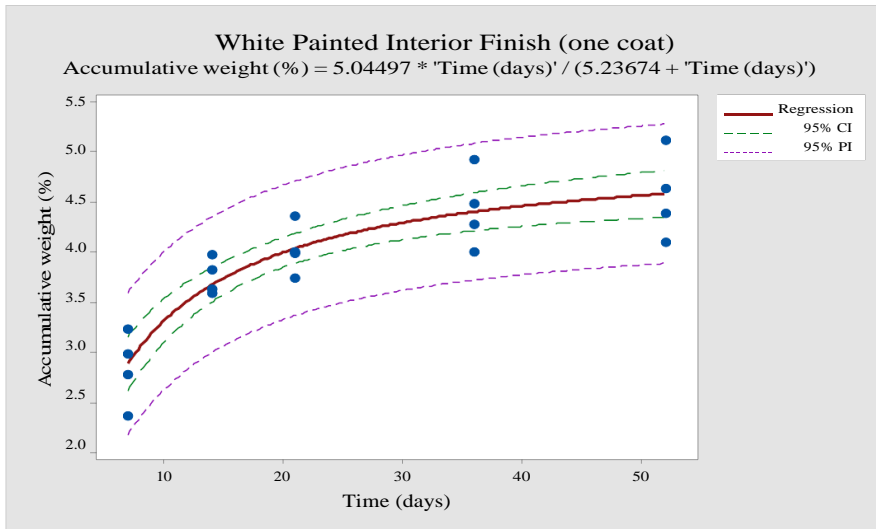
Final SSE 2.86212

DFE 16

MSE 0.178882

S 0.422945

Fitted Line: Accumulative weight (%) versus Time (days)



Nonlinear Regression: Accumulative weight (%) = H2O * ... s' / (T + ...

Method

Gauss-Newton

Algorithm

200

Max iterations

Tolerance

0.00001

Starting Values for Parameters

Parameter

Value

H2O

1

T

1

Constraints on Parameters

0 < H2O

0 < T

Equation

Accumulative weight (%) = 5.04497 * 'Time (days)' / (5.23674 + 'Time (days)')

Parameter Estimates

Parameter

Estimate

SE Estimate

H2O

5.04497

0.0011874

T

5.23674

0.004711

Accumulative weight (%) = H2O * 'Time (days)' / (T + 'Time (days)')

Lack of Fit

Source

DF

SS

MS

F

P

Error

18

1.74139

0.096744

Lack of Fit

3

0.03556

0.011853

0.1

0.956

Pure Error

15

1.70583

0.113722

Summary

Iterations

10

Final SSE

1.74139

DFE

18

MSE

0.0967439

S

0.311037

Fitted Line: Accumulative weight (%) versus Time (days)

Appendix C – General linear model of H₂O_{max} with Tukey comparison

General Linear Model: H₂O_{max} versus Density (g/cm³), Temperature (°C)

Method

Factor coding (-1, 0, +1)

Factor Information

Factor	Type	Levels	Values
Density (g/cm ³)	Fixed	2	0.335, 0.430
Temperature (°C)	Fixed	2	20, 40

Analysis of Variance

Source	DF	Adj SS	Adj MS	F-Value	P-Value
Density (g/cm ³)	1	4.8173	4.81726	14.42	0.004
Temperature (°C)	1	2.2432	2.24320	6.71	0.029
Error	9	3.0069	0.33410		
Lack-of-Fit	1	0.0113	0.01129	0.03	0.866
Pure Error	8	2.9956	0.37445		
Total	11	10.0673			

Model Summary

S	R-sq	R-sq(adj)	R-sq(pred)
0.578012	70.13%	63.50%	46.90%

Coefficients

Term	Coef	SE Coef	T-Value	P-Value	VIF
Constant	12.338	0.167	73.94	0.000	
Density (g/cm ³) 0.335	-0.634	0.167	-3.80	0.004	1.00
Temperature (°C) 20	0.432	0.167	2.59	0.029	1.00

Regression Equation

$$\text{H}_2\text{O} = 12.338 - 0.634 \text{ Density (g/cm}^3\text{)}_{0.335} + 0.634 \text{ Density (g/cm}^3\text{)}_{0.430} + 0.432 \text{ Temperature (}^\circ\text{C)}_{20} - 0.432 \text{ Temperature (}^\circ\text{C)}_{40}$$

Comparisons for H₂O_{max}

Tukey Pairwise Comparisons: Density

Grouping Information Using the Tukey Method and 95% Confidence

Density (g/cm ³)	N	Mean	Grouping
0.430	6	12.9719	A
0.335	6	11.7047	B

Means that do not share a letter are significantly different.

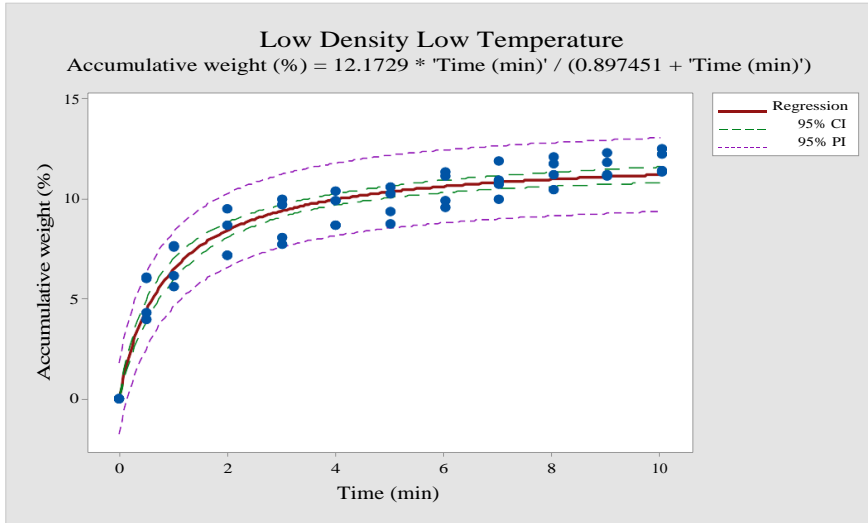
Tukey Pairwise Comparisons: Temperature (°C)

Grouping Information Using the Tukey Method and 95% Confidence

Temperature (°C)	N	Mean	Grouping
20	6	12.7706	A
40	6	11.9059	B

Means that do not share a letter are significantly different.

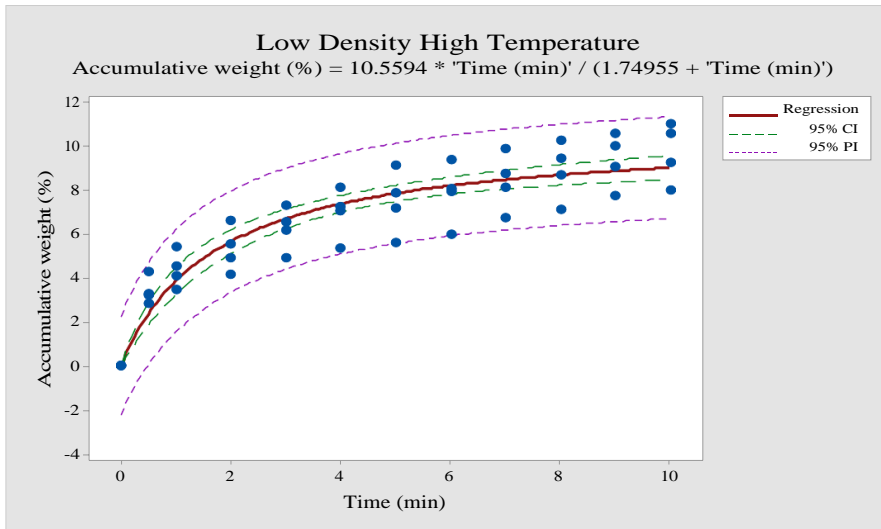
Appendix D – Average Minitab results for density and temperature



Nonlinear Regression: Accumulative weight (%) = H2O * ... n)' / (T + ...

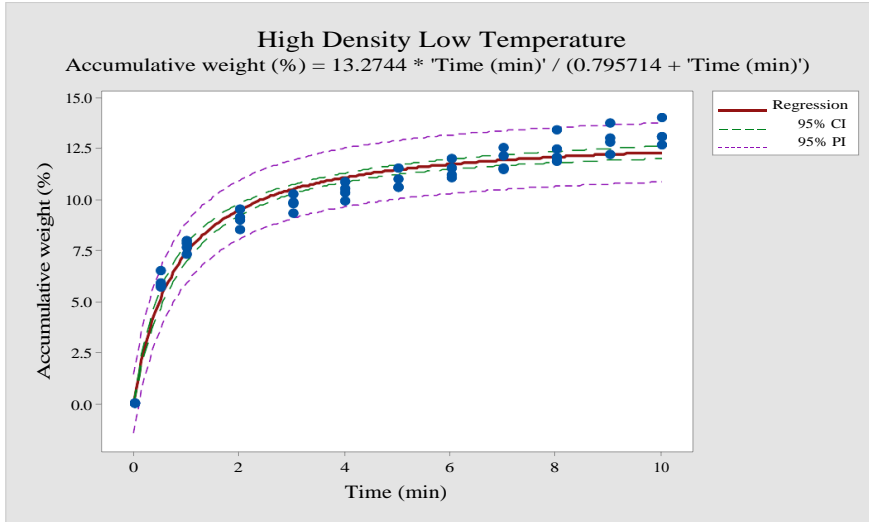
Method	Gauss-Newton				
Algorithm	200				
Max iterations	0.00001				
Tolerance					
Starting Values for Parameters					
Parameter	Value				
H2O	1				
T	1				
Constraints on Parameters					
0 < H2O					
0 < T					
Equation	Accumulative weight (%) = 12.1729 * 'Time (min)' / (0.897451 + 'Time (min)')				
Parameter Estimates					
Parameter	Estimate	SE Estimate			
H2O	12.1729	0.0000016			
T	0.8975	0.0458194			
Accumulative weight (%) = H2O * 'Time (min)' / (T + 'Time (min)')					
Lack of Fit					
Source	DF	SS	MS	F	P
Error	46	36.3477	0.79017		
Lack of Fit	10	10.1168	1.01168	1.39	0.225
Pure Error	36	26.2309	0.72864		
Summary					
Iterations	10				
Final SSE	36.3477				
DFE	46				
MSE	0.790168				
S	0.888914				

Fitted Line: Accumulative weight (%) versus Time (min)



Nonlinear Regression: Accumulative weight (%) = H2O * ... n' / (T + ...

Method					
Algorithm	Gauss-Newton				
Max iterations	200				
Tolerance	0.00001				
Starting Values for Parameters					
Parameter	Value				
H2O	1				
T	1				
Constraints on Parameters					
0 < H2O					
0 < T					
Equation	Accumulative weight (%) = 10.5594 * 'Time (min)' / (1.74955 + 'Time (min)')				
Parameter Estimates					
Parameter	Estimate	SE Estimate			
H2O	10.5594	0.0000148			
T	1.7495	0.0598496			
Accumulative weight (%) = H2O * 'Time (min)' / (T + 'Time (min)')					
Lack of Fit					
Source	DF	SS	MS	F	P
Error	46	57.1372	1.24211		
Lack of Fit	10	11.3717	1.13717	0.89	0.548
Pure Error	36	45.7656	1.27127		
Summary					
Iterations	10				
Final SSE	57.1372				
DFE	46				
MSE	1.24211				
S	1.1145				
Fitted Line: Accumulative weight (%) versus Time (min)					



Nonlinear Regression: Accumulative weight (%) = H2O * ... n' / (T + ...

Method

Gauss-Newton

Algorithm

200

Max iterations

Tolerance

0.00001

Starting Values for Parameters

Parameter

Value

H2O

1

T

1

Constraints on Parameters

0 < H2O

0 < T

Equation

Accumulative weight (%) = 13.2744 * Time (min)' / (0.795714 + Time (min)')

Parameter Estimates

Parameter

Estimate

SE Estimate

H2O

13.2744

0.0000004

T

0.7957

0.0325474

Accumulative weight (%) = H2O * Time (min)' / (T + Time (min)')

Lack of Fit

Source

DF

SS

MS

F

P

Error

46

22.6418

0.49221

7.18

0

Lack of Fit

10

15.0792

1.50792

0.21007

Pure Error

36

7.5626

Summary

Iterations

11

Final SSE

22.6418

DFE

46

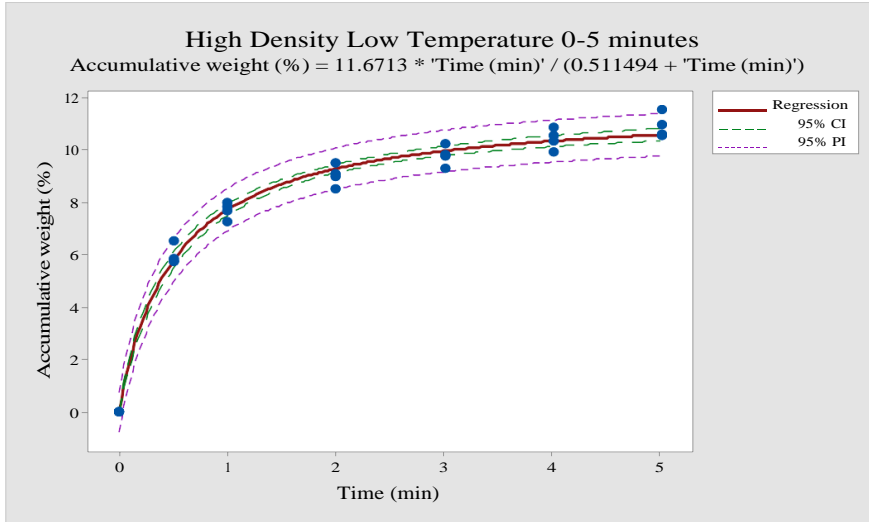
MSE

0.492214

S

0.701579

Fitted Line: Accumulative weight (%) versus Time (min)



Nonlinear Regression: Accumulative weight (%) = H2O * ... n' / (T + ...

Method

Algorithm

Gauss-Newton

Max iterations

200

Tolerance

0.00001

3 cases with missing values were not used.

Starting Values for Parameters

Parameter

Value

H2O

1

T

1

Constraints on Parameters

0 < H2O

0 < T

Equation

Accumulative weight (%) = 11.6713 * Time (min)' / (0.511494 + Time (min)')

Parameter Estimates

Parameter

Estimate

SE Estimate

H2O

11.6713

0.0000016

T

0.5115

0.0226079

Accumulative weight (%) = H2O * Time (min)' / (T + Time (min)')

Lack of Fit

Source

DF

SS

MS

F

P

Error

26

3.68001

0.141539

Lack of Fit

5

0.97908

0.195815

1.52

0.225

Pure Error

21

2.70093

0.128616

Summary

Iterations

6

Final SSE

3.68001

DFE

26

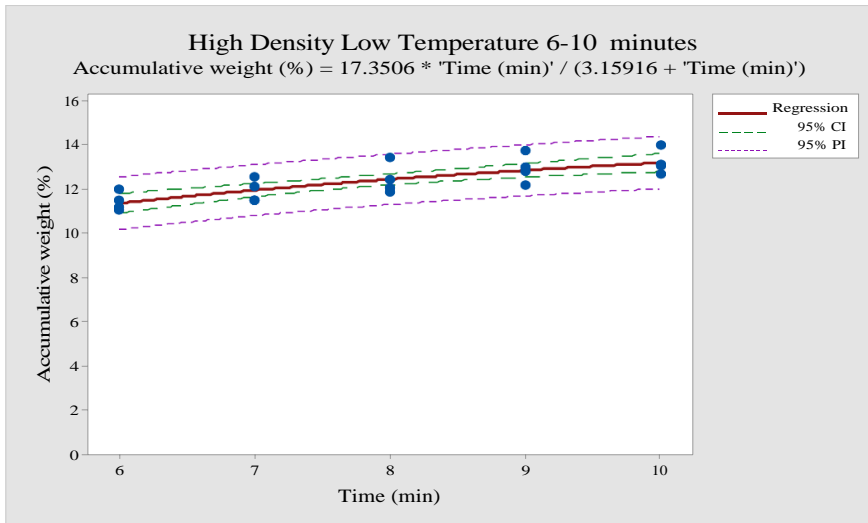
MSE

0.141539

S

0.376216

Fitted Line: Accumulative weight (%) versus Time (min)



Nonlinear Regression: Accumulative weight (%) = H2O * ... n' / (T + ...

Method

Gauss-Newton

Algorithm

200

Max iterations

0.00001

Tolerance

Starting Values for Parameters

Parameter

Value

H2O

1

T

1

Constraints on Parameters

0 < H2O

0 < T

Equation

Accumulative weight (%) = 17.3506 * Time (min)' / (3.15916 + Time (min)')

Parameter Estimates

Parameter

Estimate

SE Estimate

H2O

17.3506

0

T

3.1592

0.0347589

Accumulative weight (%) = H2O * Time (min)' / (T + Time (min)')

Lack of Fit

Source

DF

SS

MS

F

P

Error

18

4.90866

0.272703

Lack of Fit

3

0.04699

0.015662

0.05

0.985

Pure Error

15

4.86167

0.324111

Summary

Iterations

10

Final SSE

4.90866

DFE

18

MSE

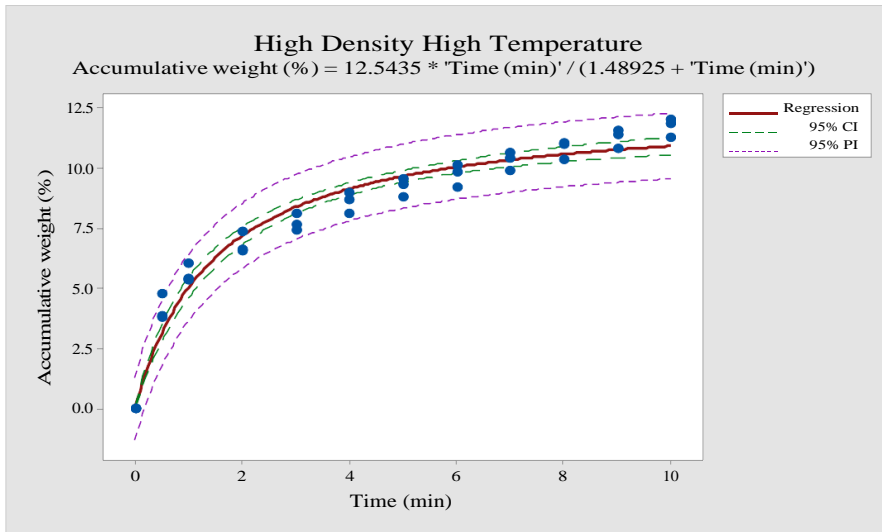
0.272703

S

0.52221

* WARNING * Some parameter estimates are highly correlated. Consider simplifying the expectation function or transforming predictors or parameters to reduce collinearities.

Fitted Line: Accumulative weight (%) versus Time (min)



Nonlinear Regression: Accumulative weight (%) = H2O * ... n' / (T + ...

Method

Gauss-Newton

Algorithm

200

Max iterations

0.00001

Tolerance

Starting Values for Parameters

Parameter

Value

H2O

1

T

1

Constraints on Parameters

0 < H2O

0 < T

Equation

Accumulative weight (%) = 12.5435 * Time (min)' / (1.48925 + Time (min)')

Parameter Estimates

Parameter

Estimate

SE Estimate

H2O

12.5435

0.0000012

T

1.4893

0.035971

Accumulative weight (%) = H2O * Time (min)' / (T + Time (min)')

Lack of Fit

Source

DF

SS

MS

F

P

Error

34

14.1349

0.41573

Lack of Fit

10

10.1739

1.01739

6.16

0

Pure Error

24

3.961

0.16504

Summary

Iterations

11

Final SSE

14.1349

DFE

34

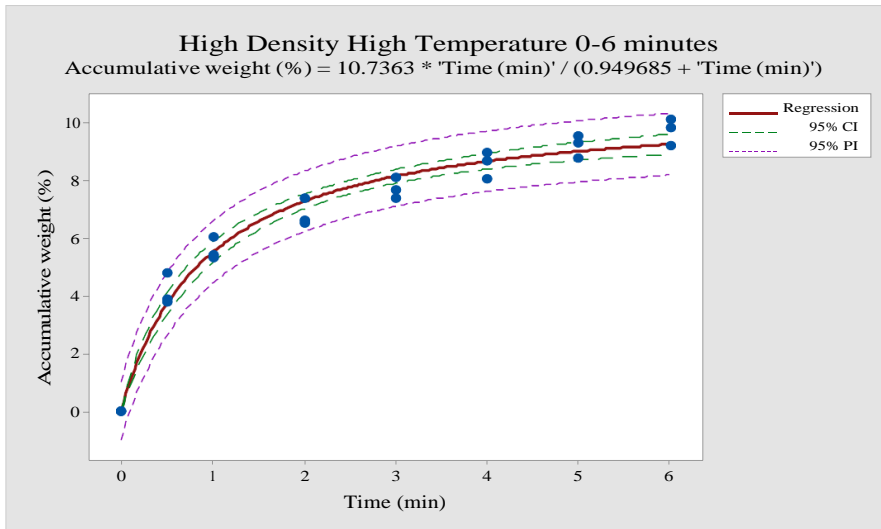
MSE

0.415733

S

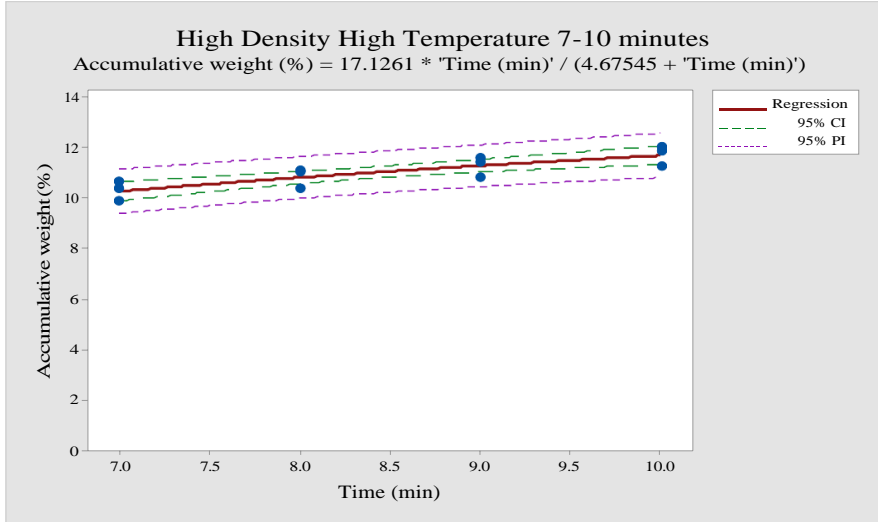
0.644773

Fitted Line: Accumulative weight (%) versus Time (min)



Nonlinear Regression: Accumulative weight (%) = H2O * ... n' / (T + ...

Method	Gauss-Newton				
Algorithm	200				
Max iterations	0.00001				
Tolerance	8 cases with missing values were not used.				
Starting Values for Parameters	Parameter Value				
Parameter	Value				
H2O	1				
T	1				
Constraints on Parameters	0 < H2O				
	0 < T				
Equation	Accumulative weight (%) = 10.7363 * Time (min)' / (0.949685 + Time (min)')				
Parameter Estimates	Parameter Estimate SE Estimate				
H2O	10.7363	0.0000071			
T	0.9497	0.041719			
Accumulative weight (%) = H2O * Time (min)' / (T + Time (min)')					
Lack of Fit					
Source	DF	SS	MS	F	P
Error	22	5.26163	0.239165		
Lack of Fit	6	2.5087	0.418116	2.43	0.073
Pure Error	16	2.75294	0.172059		
Summary					
Iterations	8				
Final SSE	5.26163				
DFE	22				
MSE	0.239165				
S	0.489045				
Fitted Line: Accumulative weight (%) versus Time (min)					



Nonlinear Regression: Accumulative weight (%) = H2O * ... n' / (T + ...

Method	Gauss-Newton
Algorithm	
Max iterations	200
Tolerance	0.00001
Starting Values for Parameters	
Parameter	Value
H2O	1
T	1

Constraints on Parameters

0 < H2O

0 < T

Equation

Accumulative weight (%) = 17.1261 * Time (min)' / (4.67545 + Time (min)')

Parameter Estimates

Parameter	Estimate	SE Estimate
H2O	17.1261	0.0000001
T	4.6754	0.0131814

Accumulative weight (%) = H2O * Time (min)' / (T + Time (min)')

Lack of Fit

Source	DF	SS	MS	F	P
Error	10	1.21448	0.121448		
Lack of Fit	2	0.0064	0.0032	0.02	0.979
Pure Error	8	1.20808	0.15101		
Summary					
Iterations	7				
Final SSE	1.21448				
DFE	10				
MSE	0.121448				
S	0.348494				

* WARNING * Some parameter estimates are highly correlated. Consider simplifying the expectation function or transforming predictors or parameters to reduce collinearities.

Fitted Line: Accumulative weight (%) versus Time (min)

Appendix E – One-way ANOVA analysis of $T_{1/2}$ with Tukey comparison

One-way ANOVA: $T_{1/2}$ (min) versus Temperature ($^{\circ}\text{C}$)

Method

Null hypothesis	All means are equal
Alternative hypothesis	Not all means are equal
Significance level	$\alpha = 0.05$

Equal variances were assumed for the analysis.

Factor Information

Factor	Levels	Values
Temperature ($^{\circ}\text{C}$)	2	20, 40

Analysis of Variance

Source	DF	Adj SS	Adj MS	F-Value	P-Value
Temperature ($^{\circ}\text{C}$)	1	2.0202	2.02024	29.57	0.000
Error	10	0.6833	0.06833		
Total	11	2.7035			

Model Summary

S	R-sq	R-sq(adj)	R-sq(pred)
0.261401	74.73%	72.20%	63.60%

Means

Temperature ($^{\circ}\text{C}$)	N	Mean	StDev	95% CI
20	6	0.8086	0.1736	(0.5708, 1.0464)
40	6	1.629	0.326	(1.391, 1.867)

Pooled StDev = 0.261401

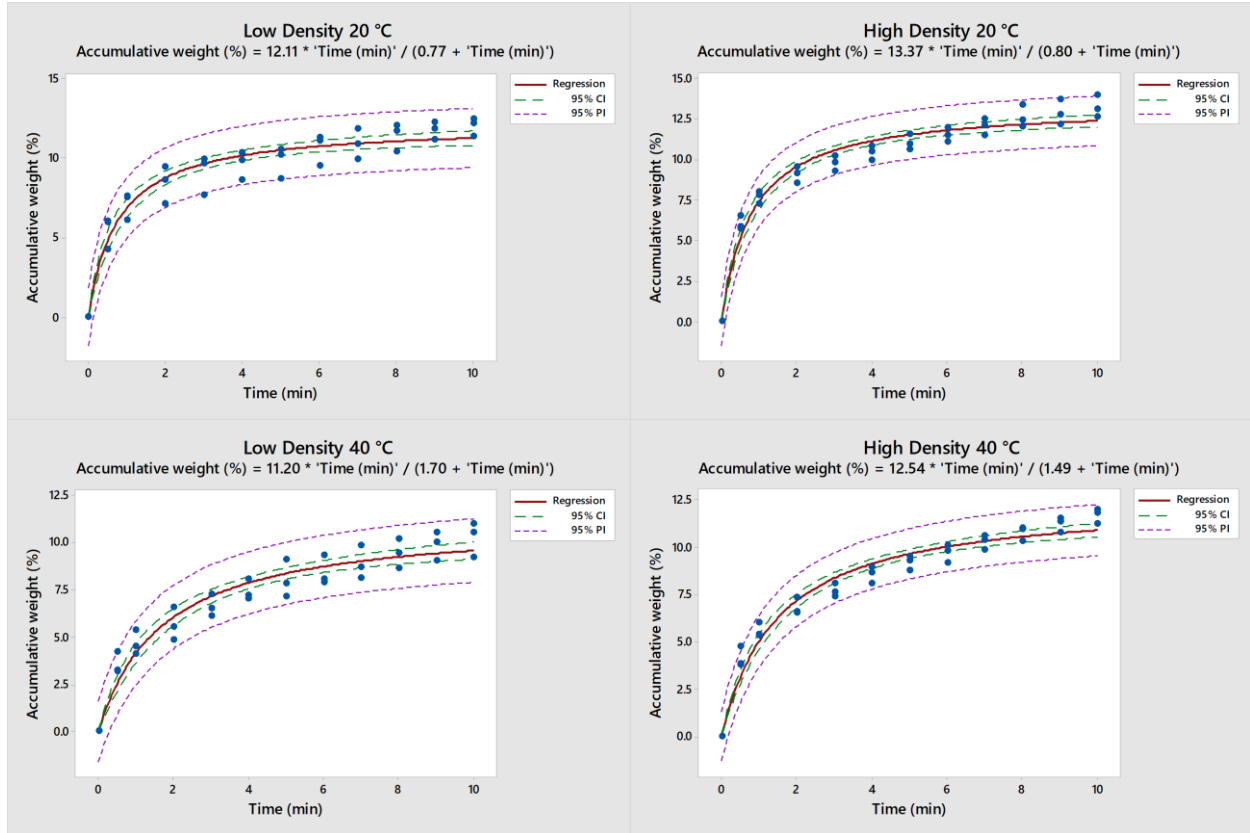
Tukey Pairwise Comparisons

Grouping Information Using the Tukey Method and 95% Confidence

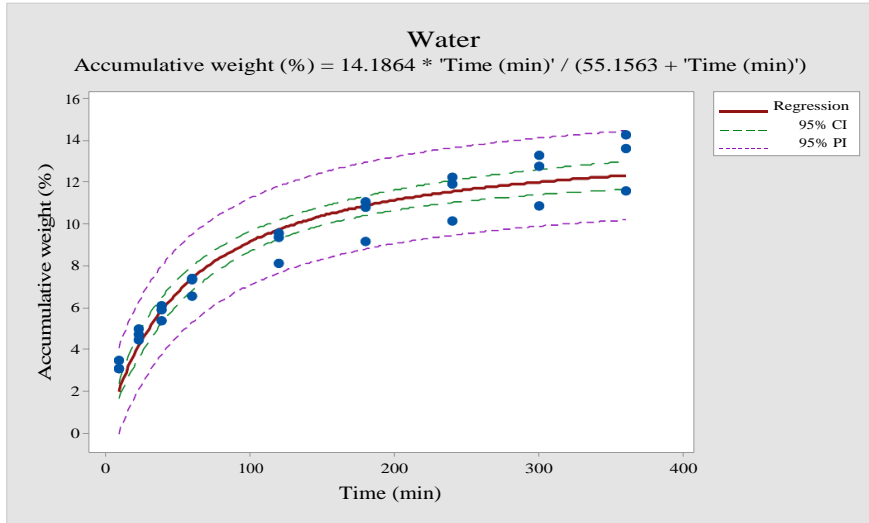
Temperature ($^{\circ}\text{C}$)	N	Mean	Grouping
40	6	1.629	A
20	6	0.8086	B

Means that do not share a letter are significantly different.

Appendix F – Averaged saturation plots

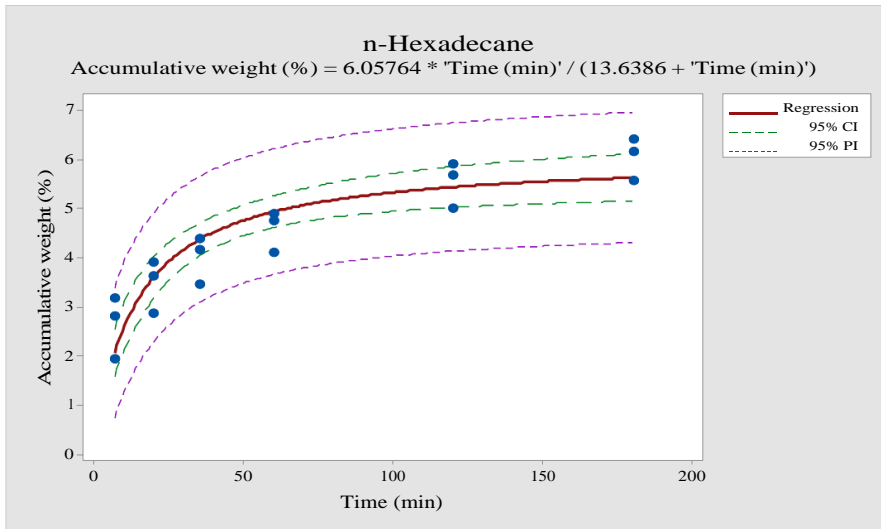


Appendix G – Individual Minitab results for water and organic solvents



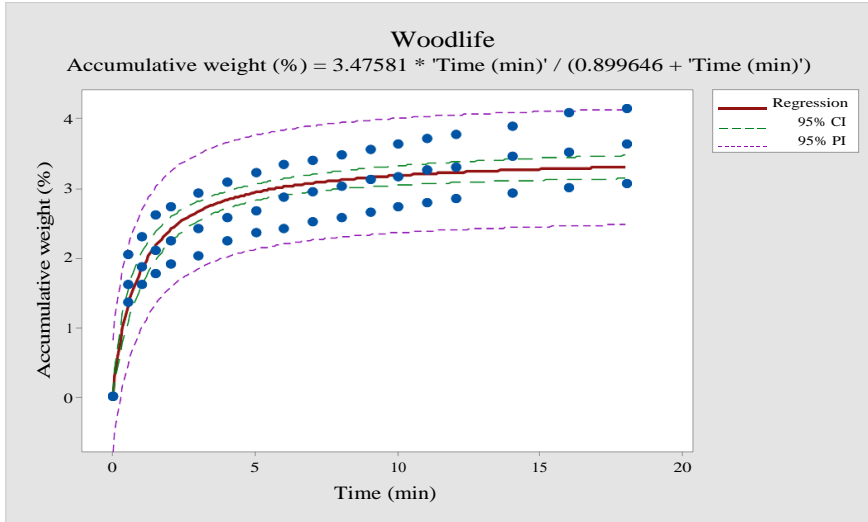
Nonlinear Regression: Accumulative weight (%) = H2O * ... n)' / (T + ...

Method	Gauss-Newton				
Algorithm	200				
Max iterations	0.00001				
Tolerance					
Starting Values for Parameters					
Parameter	Value				
H2O	1				
T	1				
Constraints on Parameters					
0 < H2O					
0 < T					
Equation	Accumulative weight (%) = 14.1864 * Time (min)' / (55.1563 + Time (min)')				
Parameter Estimates					
Parameter	Estimate	SE Estimate			
H2O	14.1864	0.0000004			
T	55.1563	0			
Accumulative weight (%) = H2O * Time (min)' / (T + Time (min)')					
Lack of Fit					
Source	DF	SS	MS	F	P
Error	25	23.9417	0.95767		
Lack of Fit	7	10.0629	1.43755	1.86	0.136
Pure Error	18	13.8788	0.77105		
Summary					
Iterations	11				
Final SSE	23.9417				
DFE	25				
MSE	0.957668				
S	0.978605				
Fitted Line: Accumulative weight (%) versus Time (min)					



Nonlinear Regression: Accumulative weight (%) = $H2O * \dots n' / (T + \dots$

Method					
Algorithm	Gauss-Newton				
Max iterations	200				
Tolerance	0.00001				
6 cases with missing values were not used.					
Starting Values for Parameters					
Parameter	Value				
H2O	1				
T	1				
Constraints on Parameters					
0 < H2O					
0 < T					
Equation					
Accumulative weight (%) = $6.05764 * \text{Time (min)} / (13.6386 + \text{Time (min)})$					
Parameter Estimates					
Parameter	Estimate	SE Estimate			
H2O	6.0576	0.0007305			
T	13.6386	0.0000036			
Accumulative weight (%) = $H2O * \text{Time (min)} / (T + \text{Time (min)})$					
Lack of Fit					
Source	DF	SS	MS	F	P
Error	16	5.45128	0.340705		
Lack of Fit	4	2.39438	0.598594	2.35	0.113
Pure Error	12	3.0569	0.254742		
Summary					
Iterations	11				
Final SSE	5.45128				
DFE	16				
MSE	0.340705				
S	0.583699				
Fitted Line: Accumulative weight (%) versus Time (min)					



Nonlinear Regression: Accumulative weight (%) = H2O * ... n' / (T + ...

Method

Gauss-Newton

Algorithm

200

Max iterations

Tolerance

0.00001

Starting Values for Parameters

Parameter

Value

H2O

1

T

1

Constraints on Parameters

0 < H2O

0 < T

Equation

Accumulative weight (%) = 3.47581 * Time (min)' / (0.899646 + Time (min)')

Parameter Estimates

Parameter

Estimate

SE Estimate

H2O

3.47581

0.0033447

T

0.89965

0.066005

Accumulative weight (%) = H2O * Time (min)' / (T + Time (min)')

Lack of Fit

Source

DF

SS

MS

F

P

Error

52

8.50789

0.163613

Lack of Fit

16

1.69814

0.106133

0.56

0.892

Pure Error

36

6.80975

0.18916

Summary

Iterations

9

Final SSE

8.50789

DFE

52

MSE

0.163613

S

0.404491

Fitted Line: Accumulative weight (%) versus Time (min)

REFERENCES

- (1) Calvert, J. G. Glossary of Atmospheric Chemistry Terms. *Pure Appl. Chem.* **1990**, *62* (11), 2167–2219.
- (2) Daus, B.; Wennrich, R.; Weiss, H. Sorption materials for arsenic removal from water : a comparative study. **2004**, *38*, 2948–2954.
- (3) Service, F. Wood Handbook - Wood as an Engineering Material. *WOOD HANDBOOK - WOOD AS AN ENGINEERING MATERIAL*, Centennial.; Forest Products Laboratory: Madison, WI, 2010.
- (4) Kukowski, K.; Martinská, V.; Krishnamoorthy, G.; Kubátová, A.; Kozliak, E. Diffusion of tebuconazole into softwood under ambient conditions and its distribution in freshly treated and aged wood. *Int. J. Heat Mass Transf.* **2016**, *102*, 1257–1266.
- (5) Erich, S. J. F.; Adan, O. C. G.; van der Ven, L. G. J.; Gezici-Koç, Ö.; Huinink, H. P. Bound and free water distribution in wood during water uptake and drying as measured by 1D magnetic resonance imaging. *Cellulose* **2016**, *24* (2), 535–553.
- (6) Stamm, A. J. Review of Nine Methods for Determining the Fiber Saturation Points of Wood and Wood Products. *Wood Sci.* **1971**, *4* (2), 114–128.
- (7) Popescu, C. M.; Hill, C. A. S. The water vapour adsorption-desorption behaviour of naturally aged *Tilia cordata* Mill. wood. *Polym. Degrad. Stab.* **2013**, *98* (9), 1804–1813.
- (8) Bramhall, G. Diffusion and the drying of wood. *Wood Sci. Technol.* **1995**, *29* (3), 209–215.
- (9) Sonderegger, W.; Vecellio, M.; Zwicker, P.; Niemz, P. Combined bound water and water vapour diffusion of Norway spruce and European beech in and between the principal anatomical directions. *Holzforschung* **2011**, *65* (6), 819–828.

- (10) Shi, S. Q. Diffusion model based on Fick's second law for the moisture absorption process in wood fiber-based composites: Is it suitable or not? *Wood Sci. Technol.* **2007**, *41* (8), 645–658.
- (11) Baglayeva, G.; Seames, W. S.; Frihart, C. R.; O'Dell, J.; Kozliak, E. I. Penetration of *n* - Hexadecane and Water into Wood under Conditions Simulating Catastrophic Floods. *For. Prod. J.* **2017**, *67* (3–4), 236–244.
- (12) Baglayeva, G.; Krishnamoorthy, G.; Frihart, C. R.; Seames, W. S.; O'Dell, J.; Kozliak, E. I. Modeling of *n*-hexadecane and water sorption in wood. *For. Prod. J.* **2016**, *66* (7/8), 401–412.
- (13) Murr, A.; Lackner, R. Analysis on the influence of grain size and grain layer thickness on the sorption kinetics of grained wood at low relative humidity with the use of water vapour sorption experiments. *Wood Sci. Technol.* **2018**, *52* (3), 753–776.
- (14) Kang, W.; Kang, C. W.; Chung, W. Y.; Eom, C. D.; Yeo, H. The effect of openings on combined bound water and water vapor diffusion in wood. *J. Wood Sci.* **2008**, *54* (5), 343–348.
- (15) Kumaran, M. K. Moisture Diffusivity of Building Materials from Water Absorption Measurements. *J. Therm. Envel. Build. Sci.* **1999**, *22* (4), 349–355.
- (16) Peralta, P. N.; Bangi, A. P. A nonlinear regression technique for calculating the average diffusion coefficient of wood during drying. *Wood Fiber Sci.* **2003**, *35* (3), 401–408.
- (17) Wadsö, L. Describing non-Fickian water-vapour sorption in wood. *J. Mater. Sci.* **1994**, *29* (9), 2367–2372.
- (18) Glass, S. V.; Zelinka, S. L.; Johnson, J. A. Investigation of Historic Equilibrium Moisture Content Data from the Forest Products Laboratory. *For. Prod. Lab.* **2014**, 1–37.

- (19) Johnson, K. A.; Goody, R. S. The original Michaelis constant: Translation of the 1913 Michaelis-Menten Paper. *Biochemistry* **2011**, *50* (39), 8264–8269.
- (20) Ritchie, R. J.; Prvan, T. Current Statistical Methods for Estimating the Km and Vma of Michaelis-Menten Kinetics RAYMOND. *Biochem. Educ.* **1996**, *24* (4), 196–206.
- (21) Kukowski, K.; Hatton, J.; Kozliak, E. I.; Kubátová, A. Science of the Total Environment The extent of tebuconazole leaching from unpainted and painted softwood. *Sci. Total Environ.* **2018**, *633*, 1379–1385.
- (22) Scintillation system LS 6500 Operating Instructions. Beckman Coulter, Inc.: Fullerton, CA 1992.
- (23) Robinson, J. W.; Skelly Frame, E. M.; Frame II, G. M. Undergraduate Instrumental Analysis. *UNDERGRADUATE INSTRUMENTAL ANALYSIS*, Sixth.; Marcel Dekker: New York, NY, 2005.
- (24) Minitab Statistical Software. Minitab, LLC.
- (25) Zeng, G.; Zhang, C.; Huang, G.; Yu, J.; Wang, Q.; Li, J.; Xi, B.; Liu, H. Adsorption behavior of bisphenol A on sediments in Xiangjiang River, Central-south China. *Chemosphere* **2006**, *65* (9), 1490–1499.
- (26) Miura, A.; Shiratani, E.; Yoshinaga, I.; Hitomi, T.; Hamada, K.; Takaki, K. Characteristics of the adsorption of dissolved organic matter by charcoals carbonized at different temperatures. *Japan Agric. Res. Q.* **2007**, *41* (3), 211–217.

MINITAB® and all other trademarks and logos for the Company's products and services are the exclusive property of Minitab, LLC. All other marks referenced remain the property of their respective owners. See minitab.com for more information.